UNIVERSITÀ
DI SIENA
1240

Dipartimento di Scienze mediche, chirurgiche e neuroscienze

Dottorato in *Translational and Precision Medicine*

38° Ciclo

Coordinatore Prof. Francesco Dotta

Translational Insights into T Cell Dysfunction and Precision Therapy in Idiopathic Pulmonary Fibrosis

Settore scientifico disciplinare: *MED/10*

Candidata

Sara Gangi

Department of Medical sciences, surgery and Neurosciences, Respiratory Disease and Lung Transplant Unit, University of Siena, Italy

Supervisore

Sara Gangi Firmato il 26.11.2025 12:08:56

Elena Bargagli

Department of Medical sciences, surgery and Neurosciences, Respiratory Disease and Lung Transplant Unit, University of Siena, Italy.

Co-supervisore

Laura Bergantini

Department of Medical sciences, surgery and Neurosciences, Respiratory Disease and Lung Transplant Unit, University of Siena, Italy.

Anno accademico di conseguimento del titolo di Dottore di ricerca

2024/25

Contents:

Abstract

Idiopathic pulmonary fibrosis (IPF) is a chronic, progressive interstitial lung disease characterized by irreversible fibrosis and a gradual decline in pulmonary function. Its pathogenesis involves persistent epithelial injury, aberrant tissue repair, and excessive fibrotic remodelling driven by dysregulated immune responses. Growing evidence indicates that both innate and adaptive immune cells play a central role in disease progression. Despite advances in understanding its mechanisms, current treatments—pirfenidone, nintedanib, and nerandomilast—remain limited in efficacy.

This study aimed to delineate the immunological landscape of IPF, characterize systemic T-cell dysfunction, and explore immune alterations in $CD8^+$ cells following exposure to anti–PD-1 and nintedanib. Peripheral blood mononuclear cells (PBMC) from 47 IPF patients and 8 healthy controls were analysed by multicolour flow cytometry to assess the expression of the inhibitory receptors PD-1 and TIGIT on $CD4^+$, $CD8^+$, and $CD56^+$ lymphocyte subsets. Purified $CD8^+$ T cells from 5 IPF patients and 4 healthy controls were further stimulated in vitro and treated with anti–PD-1, nintedanib, or their combination to evaluate changes in activation, proliferation, and cytotoxicity.

IPF patients exhibited a consistent upregulation and co-expression of PD-1 and TIGIT across $CD4^+$, $CD8^+$, and $CD56^+$ T-cell subsets, indicating a state of systemic immune exhaustion. In vitro, $CD8^+$ T cells showed dysregulated activation markers (CD25, CD69) and reduced cytotoxic potential (granzyme B, perforin). Neither anti–PD-1 nor nintedanib treatment restored functional competence and both maintained elevated inhibitory receptor expression, although nintedanib modestly enhanced $CD8^+$ T-cell proliferation. Combined treatment did not reverse the exhausted phenotype, suggesting persistent overlapping inhibitory mechanisms and a stable imprint of chronic dysfunction.

Overall, this PhD work reveals a marked systemic immune imbalance in IPF, characterized by persistent activation, inhibitory receptor overexpression, and functional exhaustion of T cells. The resistance of this phenotype to immunomodulatory

interventions underscores the complexity of immune dysregulation in IPF and the need for therapeutic strategies targeting multiple inhibitory pathways.

Table of abbreviation

ABCA3	ATP-Binding Cassette Subfamily A Member 3
AEC	Alveolar Epithelial Cell
AEC1	Type I Alveolar Epithelial Cell
AEC2	Type II Alveolar Epithelial Cell
ALAT	Latin American Thoracic Society
AKAP13	A Kinase Anchoring Protein 13
ATS	American Thoracic Society
BAL	Bronchoalveolar Lavage
BCR	B Cell Receptor
CD	Cluster of Differentiation
CD25	Cluster of Differentiation 25 (IL-2 receptor α chain, late activation marker)
CD56^bright	CD56 bright NK cell subset
CD56^dim	CD56 dim NK cell subset
CD69	Cluster of Differentiation 69 (early activation marker)
ci-NK	Circulating Cytotoxic NK Cell
COL	Collagen (gene/protein)
CSF1R	Colony-Stimulating Factor 1 Receptor
CT	Computed Tomography
CTL	Cytotoxic T Lymphocyte
DC	Dendritic Cell
DLCO	Diffusing Capacity for Carbon Monoxide
ECM	Extracellular Matrix
EMT	Epithelial-to-Mesenchymal Transition
EMA	European Medicines Agency
ERS	European Respiratory Society
FAK	Focal Adhesion Kinase
FGF	Fibroblast Growth Factor
FGFR	Fibroblast Growth Factor Receptor
FLT3	FMS-like Tyrosine Kinase 3
FVC	Forced Vital Capacity
Granzyme B	Cytotoxic effector protease in T cells and NK cells
HCs	Healthy Controls
HRCT	High-Resolution Computed Tomography
IFN-γ	Interferon Gamma
ICAM-1	Intercellular Adhesion Molecule 1 (CD54)
IL	Interleukin
ILC	Innate Lymphoid Cell
ILC2	Type-2 Innate Lymphoid Cell

iNKT	Invariant Natural Killer T cell
ILD	Interstitial Lung Disease
IIP	Idiopathic Interstitial Pneumonia
IPF	Idiopathic Pulmonary Fibrosis
JRS	Japanese Respiratory Society
JUN	Jun Proto-Oncogene
LAM	Lymphangioleiomyomatosis
LAMP-1	Lysosomal-associated membrane protein 1 (CD107a, degranulation marker)
MAPK	Mitogen-Activated Protein Kinase
MDSC	Myeloid-Derived Suppressor Cell
MHC	Major Histocompatibility Complex
MMP	Matrix Metalloproteinase
MUC5B	Mucin 5B
NET	Neutrophil Extracellular Trap
NK	Natural Killer
NKT-like cells	$CD3^{+}CD56^{+}$ T cells with NKT-like features
PBMC	Peripheral Blood Mononuclear Cell
PD-1	Programmed Cell Death Protein 1
PD-L1	Programmed Death-Ligand 1
PD-L2	Programmed Death-Ligand 2
PDGFR	Platelet-Derived Growth Factor Receptor
PDE4B	Phosphodiesterase-4B
Perforin	Cytotoxic effector molecule
PI3K	Phosphatidylinositol 3-Kinase
PKC	Protein Kinase C
PCA	Principal Component Analysis
RTEL1	Regulator of Telomere Elongation Helicase 1
R	(if used, clarify context)
SASP	Senescence-Associated Secretory Phenotype
SFTPA2	Surfactant Protein A2
SFTPC	Surfactant Protein C
TCR	T Cell Receptor
TGF-β	Transforming Growth Factor Beta
Th	T Helper Cell
Th1	T Helper Type 1 Cell
Th2	T Helper Type 2 Cell
Th17	T Helper Type 17 Cell
TIGIT	T Cell Immunoreceptor with Ig and ITIM Domains
TIMP	Tissue Inhibitor of Metalloproteinase
TINF2	TERF1-Interacting Nuclear Factor 2
TOLLIP	Toll-Interacting Protein
TNF	Tumour Necrosis Factor
Treg	Regulatory T Cell
TERT	Telomerase Reverse Transcriptase

TERC	Telomerase RNA Component
UPR	Unfolded Protein Response
UIP	Usual Interstitial Pneumonia
VEGFR	Vascular Endothelial Growth Factor Receptor
ZAP-70	Zeta-chain-associated protein kinase 70

List of tables

List of figures

4. Mechanisms and signals involved in the development of pulmonary fibrosis and therapeutic targets.
5. **Pathophysiological Cascade Leading to Pulmonary Fibrosis**. Repetitive epithelial injury triggers dysregulated repair responses in the lung. Damaged alveolar epithelial cells release inflammatory and fibrotic mediators that recruit immune cells and activate fibroblasts. Persistent activation leads to excessive myofibroblast differentiation and extracellular matrix deposition, causing scarring, impaired gas exchange, and progressive respiratory decline.
6. **Role for immune dysregulation in promoting the development of pulmonary fibrosis.** Profibrotic responses are driven by M2 macrophages, Th17 cells, CD8+ T cells, and potentially Tregs, whereas Th1 cells and TRM CD4+ T cells may play a protective role against fibrosis.
7. **Differentiation of helper T cell subsets from naive $CD4^+$ T cells mediated by cytokines and co-signals.** Various cytokines and co-stimulatory signals from antigen-presenting cells drive the differentiation of distinct T cell subsets, including Th1, Th2, Th17, Th9, Th22, Tfh, and Treg cells. These subsets, regulated by key transcription factors such as T-bet, GATA3, RORγt, STATs, and FoxP3, coordinate immune responses to pathogens, self-antigens, and tumors.
8. **Structure of PD-1 and its ligands PD-L1/2.** (A) PD-1 consists of two extracellular immunoglobulin-like domains (IgV and IgC), a transmembrane segment, and an intracellular tail containing ITIM and ITSM signalling motifs. (B) Its ligands, PD-L1 and PD-L2, share a similar extracellular immunoglobulin-like structure.
9. **The PD-1/PD-L1 axis as a driver of fibrotic remodeling in IPF through multifaceted intercellular and signaling interactions.** The PD-1/PD-L1 axis contributes to idiopathic pulmonary fibrosis (IPF) by promoting profibrotic signaling across multiple cell types. PD-L1 upregulation enhances Th17-mediated IL-17 and TGF-β production, activates fibroblast survival and differentiation via p53, FAK, Smad3, and β-catenin pathways, and suppresses autophagy and adaptive immunity. These effects collectively drive myofibroblast proliferation, extracellular matrix accumulation, and immune

evasion, leading to progressive fibrosis.

10. **Experimental design and workflow of the study**. Phase 1 involved peripheral blood mononuclear cell (PBMC) isolation and immunophenotyping from 47 idiopathic pulmonary fibrosis (IPF) patients. In Phase 2, PBMCs from 5 IPF patients were used for $CD8^+$ T-cell isolation, followed by stimulation with or without anti-PD-1 and nintedanib, and subsequent assessment of immunophenotype, cytotoxicity, and proliferation.
11. **Isolation and storage of Human Peripheral Blood Mononuclear Cells (PBMC).**
12. **Flow cytometry gating strategy for identifying PD-1^+ and TIGIT$^+$ expression on $CD4^+$ and $CD8^+$ T cells and $CD56^+$ cells.** Peripheral blood mononuclear cells (PBMCs) were gated based on size and granularity to identify lymphocytes, followed by selection of $CD3^+$ T cells. $CD4^+$ and $CD8^+$ and $CD56^+$ cells subsets were analysed for PD-1 and TIGIT co-expression to assess activation and exhaustion profiles.
13. **Flow cytometry gating strategy for identifying $CD56^+$ subpopulation expressing PD-1 and TIGIT.** Peripheral blood mononuclear cells (PBMCs) were gated based on size and granularity to identify lymphocytes, followed by selection $CD56^+$ cells. $CD56^+$ cells subpopulation were analysed for PD-1 and TIGIT co-expression to assess activation and exhaustion profiles.
14. **Protocol of $CD8^+$ T cells isolation.** CD8+ T cells were isolated from thawed PBMCs, and their purity and viability were confirmed by flow cytometry. Cells were then seeded, and the following day, stimulated and treated with or without anti-PD-1 and nintedanib.
15. On the left, characteristics of the monoclonal antibodies used for spectral flow cytometric analysis, including clone, fluorochrome, and manufacturer. On the right, the spectrum viewer of monoclonal antibodies.
16. **Flow cytometry gating strategy for identifying $CD8^+$ expressing activation markers (CD25 and CD69), immune checkpoints (PD-1 and TIGIT), cytotoxicity markers (granzyme and perforin), degranulation marker (LAMP-1), adhesion marker (ICAM-1)**. Gating strategy for Live cells and singlets were gated out using forward and side scatter properties. Sub-gating for

population that are simultaneously expressing CD3 and CD8 were performed to assess CD25, CD69, PD-1, TIGIT, Granzyme, Perforin, LAMP-1 and ICAM-1expression with CD8 cells.

17. **Increased PD-1 and TIGIT surface expression in IPF $CD4^+$, $CD8^+$ and $CD56^+$ T cells.** PD-1 and TIGIT expression in cells from IPF patients compared to Healthy Controls (HCs, n= 8; IPF, n= 47). $^*p<0.005$, $^{**}p<0.01$, $^{***}p<0.001$, $^{****}p<0.0001$.
18. **Enhanced TIGIT and PD-1 Expression in CD56^bright, CD56^dim, and NKT Cells in Idiopathic Pulmonary Fibrosis.** TIGIT and PD-1 expression in cells from IPF patients compared to Healthy Controls (HCs, n= 8; IPF, n= 47). $^*p<0.005$, $^{**}p<0.01$, $^{***}p<0.001$, $^{****}p<0.0001$.
19. **Correlation matrix of immune checkpoint expression in T cell subsets of IPF patients.** Spearman correlation matrix illustrating the pairwise correlations between frequencies of $CD4^+$, $CD8^+$, and $CD56^+$ T cells, including subsets expressing the immune checkpoints PD-1 and TIGIT, in patients with IPF (Fig. A) and HC (Fig. B). The colour scale in the legend indicates the strength and direction of correlation (Spearman's rho).
20. **Principal component analysis (PCA) of CD8 T cells across treatments and disease status. A:** Individual samples from unstimulated (UNSTIM), nintedanib (NINT), anti-PD-1, and combined anti-PD-1 + NINT conditions in healthy controls (HCs) and IPF patients, projected onto the first two principal components (PC1: 34.9%, PC2: 22.5%), explaining 57.4% of total variance. Samples cluster primarily by treatment and disease status. **B:** Biplot showing key variables driving separation, including CD69, PD-1, TIGIT, ICAM-1, Granzyme B, Perforin, and LAMP-1.
21. **Principal component analysis (PCA) of $CD8^+$ T cells isolated from idiopathic pulmonary fibrosis (IPF) patients (n = 5) and healthy controls (HCs, n = 4) under four experimental conditions**: unstimulated (UNSTIM), nintedanib (NINT), anti-PD-1, and combined anti-PD-1 + nintedanib (anti-PD-1 + NINT). Each point represents an individual donor, and 95% confidence ellipses denote the distribution of each group. Biplots display the direction and magnitude of the

variables contributing most strongly to sample separation. Percentages on the axes indicate the proportion of variance explained by each principal component.

22. **Hierarchical clustering and heatmap analysis of $CD8^+$ T-cell markers in IPF patients (n = 5) and HCs, n = 4 across four experimental conditions (unstimulated, nintedanib, anti-PD-1, and anti-PD-1 + nintedanib). A:** Dendrogram of marker clustering based on Euclidean distance, highlighting four main clusters corresponding to cytotoxic/degranulation (LAMP-1, Granzyme B, Perforin), activation/adhesion (ICAM-1, CD25, CD69), and inhibitory checkpoint (PD-1, TIGIT) signatures. **B:** Heatmap of normalized marker expression across samples. Each column represents an individual donor in each condition; colour intensity reflects relative expression levels (yellow = low, dark red = high). IPF and HC groups exhibit distinct clustering patterns, consistent with differential activation states.
23. Fig.23 **Activation markers (CD25 and CD69) in $CD8^+$ T-cell from IPF patients and healthy controls under different treatment conditions.** Box-and-whisker plots (showing median, interquartile range, and individual data points) depict the frequency of $CD25^+$ (on the top, A.) and $CD69^+$ (on the bottom, B.) $CD8^+$ T cells isolated from IPF patients (n = 5) and healthy controls (HCs; n = 4) under four conditions: unstimulated (Unstim), anti-PD1, Nintedanib (Nint), and combined anti-PD1 + Nintedanib. Statistical significance was assessed using the Friedman test with Dunn's multiple comparison test ($p < 0.05$).
24. Fig.24 **Exhaustion markers (PD-1 and TIGIT) in $CD8^+$ T cells from IPF and healthy controls.** Box-and-whisker plots with overlaid data points represent $PD\text{-}1^+$ (top, A.) and $TIGIT^+$ (bottom, B.) $CD8^+$ T-cell frequencies across treatment conditions. Statistical significance was assessed using the Friedman test with Dunn's multiple comparison test ($p < 0.05$).
25. **Cytotoxicity markers (Granzyme B, Perforin, and LAMP-1) in $CD8^+$ T cells from IPF and healthy controls.** Box-and-whisker plots show the distribution of Granzyme B^+ (A.), $Perforin^+$(B.), and $LAMP\text{-}1^+$ (C.) $CD8^+$ T cells across the four treatment conditions. Statistical significance was assessed using the Friedman test with Dunn's multiple comparison test ($p < 0.05$).

26. **Adhesion marker (ICAM-1) in CD8$^+$ T cells from IPF and HCs**. Box-and-whisker plots with individual data points represent ICAM-1$^+$CD8$^+$ T-cell frequencies under the four experimental conditions. Statistical significance was assessed using the Friedman test with Dunn's multiple comparison test ($p < 0.05$).
27. **Anti-PD-1, nintedanib, and their combination modulate the cytotoxic activity of CD8+ T cells in IPF and healthy controls (HCs).** Cytotoxicity of CD8$^+$ T cells from (A-B) IPF patients and (C-D) HCs was measured following 48 hours of treatment with anti-PD-1, nintedanib, or their combination. On the left, points & connecting lines represent individual cell responses over time. On the right, histograms depict the mean cytotoxicity levels for each treatment group.
28. Fig.28 **Anti-PD-1, nintedanib, and their combination modulate the Proliferation of CD8$^+$ T cells in IPF and healthy controls (HCs).** Proliferation of CD8+ T cells from (A-B) IPF patients and (C-D) healthy controls (HCs) after 48 hours of treatment with anti-PD-1, nintedanib, or their combination

CHAPTER 1: Introduction

1.1 Interstitial lung disease (ILD)

Interstitial lung diseases (ILD) encompass a diverse and extensive range of disorders, both nosological and non-neoplastic in nature. These diseases are characterized by widespread lung infiltration resulting from pulmonary inflammation, which can progress into irreversible fibrosis and lead to respiratory failure. In 2002, the Consensus Statement from the American Thoracic Society and the European Respiratory Society (ATS/ERS) categorized ILD into four distinct groups based on their etiopathogenesis: 1) Known causes, including secondary conditions such as collagen vascular diseases, drug exposure, irritants, and environmental or occupational factors; 2) Idiopathic interstitial pneumonia (IIP); 3) Granulomatous lung diseases; and 4) Other forms defined by specific morphological features, such as Lymphangioleiomyomatosis (LAM), Langerhans cell histiocytosis, and eosinophilic pneumonia, Fig 1. This framework was refined in the 2013 revision of the international multidisciplinary classification, which expanded IIP subtypes and introduced unclassifiable forms (1). The most recent 2025 ATS/ERS update extended it beyond idiopathic form to include secondary interstitial pneumonia, distinguishing fibrotic from non-fibrotic patterns, and incorporating diagnostic confidence levels (2).

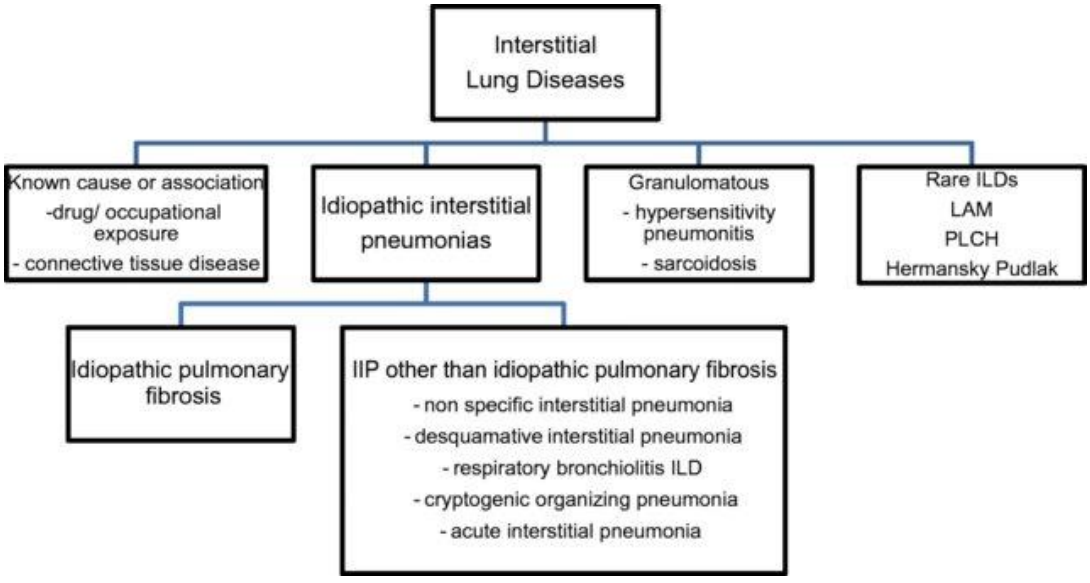

Figure 1. Interstitial lung disease classification (3)

Idiopathic interstitial pneumonias (IIPs) are a diverse group of non-cancerous diseases with an unknown cause, primarily affecting the pulmonary interstitium—the space between the epithelial and endothelial layers of the basal membranes. Pulmonary function changes in ILD typically show a restrictive deficit, caused by the reduced expansion of total lung capacity (4). Patients experience symptoms such as dyspnea, tachypnea, crackles, and possibly cyanosis, along with other signs of restriction. Additional findings include decreased diffusion capacity for carbon monoxide (DLCO), reduced lung volume, and impaired compliance during respiratory tests (5).

1.2. Idiopathic pulmonary fibrosis: Definition

Idiopathic pulmonary fibrosis (IPF) is a chronic, fibrosing interstitial pneumonia of unknown aetiology, characterized by radiological and histological patterns consistent with usual interstitial pneumonia (UIP). It predominantly affects older adults, is marked by the progressive deterioration of dyspnoea and pulmonary function, and is associated with a poor prognosis (6). This debilitating disease significantly impacts both the quality of life and life expectancy of affected individuals, with a median survival of approximately three years (7). Approximately 20-30% of patients with interstitial lung diseases are diagnosed with IPF. Although it is regarded as the most prevalent form of idiopathic interstitial pneumonia, predominantly affects men with a mean age of 65 at diagnosis The incidence and prevalence of IPF in Europe to range from 0.22 to 2.8 and 1.25 to 8.2 cases per 100,000 individuals, respectively (8).

1.3 Risk factors for IPF and genetic predisposition

Although IPF is classified as a disease of unknown aetiology, its pathogenesis is influenced by a combination of genetic predispositions and environmental factors. Demographic and environmental risk factors play a crucial role in IPF. The disease shows a strong positive correlation with advancing age, with older individuals exhibiting higher incidence and mortality, likely due to mechanisms involving cellular senescence and impaired tissue repair (9). IPF occurs more frequently in males, although females may experience slower progression and better survival (10). Environmental exposures,

particularly **cigarette smoking**—notably beyond 20 pack-years—are strongly associated with disease onset and accelerated lung function decline (11). Additionally, occupational exposure to **metal and wood dust**, **crystalline silica**, and **organic pollutants** increases IPF risk through chronic immune activation and fibrotic remodelling, with susceptibility influenced by exposure duration, particle size, and host factors (12). The following table includes the main genetic mutations associated to the development of pulmonary fibrosis.

Table 1. main genetic mutations associated to the development of pulmonary fibrosis

Genetic:	Description
MUC5B Promoter Polymorphism (rs35705950):	The minor allele of rs35705950 increases IPF risk, with a 3-fold risk in heterozygotes and a 7-fold risk in homozygotes. This variant enhances MUC5B expression, impairing mucociliary clearance, though its exact role in disease pathogenesis is unclear. (13) (14)
	Three variants in TOLLIP are associated with increased IPF risk in Europeans, linked to reduced TOLLIP expression, potentially affecting immune responses and disease progression. (14)
Surfactant processing	In families with pulmonary fibrosis, rare genetic variants in genes involved in surfactant processing, such as SFTPC, SFTPA2, and ABCA3, have been identified. (15) (16)
Fibrotic signal	The single nucleotide polymorphism rs62025270 has been associated with an increased risk of IPF and with increased expression of AKAP13 in the lung.
	A Kinase Anchoring Protein 13 (AKAP13) is a A-kinase anchoring protein, it is an essential enzyme in the cAMP signalling cascade. It acts as a multivalent scaffold protein with a unique (GEF) domain, involved in profibrotic

	signalling pathways. (17)
Telomerase maintenance	Variants in telomere maintenance genes (TERT, TERC, PARN, RTEL1, DKC1, and TINF2) are linked to both familial and sporadic pulmonary fibrosis. These variants result in telomere shortening and accelerated cellular senescence, which is believed to contribute to impaired epithelial repair. (14) (18)

1.4 Diagnosis

Diagnosis of IPF is established through the integration of radiological and histological findings. The guidelines were formulated in 2011 by the American Thoracic Society (ATS), European Respiratory Society (ERS), Japanese Respiratory Society (JRS), and Latin American Thoracic Society (ALAT) (19) Chest high-resolution CT (HRCT) is critical for diagnosing IPF. A definite or probable usual interstitial pneumonia (UIP) pattern on HRCT, characterized by subpleural and basal fibrosis, honeycombing, and traction bronchiectasis, strongly supports the diagnosis. A multidisciplinary approach, including clinical, radiological, and histopathological input, enhances diagnostic confidence. If HRCT is unclear, further tests like BAL, surgical biopsy, or transbronchial cryobiopsy may be used. A standardized diagnostic approach based on likelihood and confidence helps guide treatment, with ongoing re-evaluation as more data emerges (20) (21).

1.5 Current therapies

IPF remains a progressive and ultimately fatal interstitial lung disease with limited therapeutic options. Although three antifibrotic agents—pirfenidone, nintedanib and nerandomilast—have been approved for clinical use, neither therapy halts or reverses the disease. Instead, they primarily function to decelerate its progression.

Pirfenidone is a small molecule with pleiotropic effects (antifibrotic, inflammatory and antioxidants properties) thought to exert its effects by modulating transforming growth

factor-beta (TGF-β) signaling pathways, thereby inhibiting fibroblast proliferation and collagen deposition (22). It was the first antifibrotic agent to be approved for the treatment of IPF in In February 2011 by the European Commission Clinical trials that led to its approval demonstrated a significant reduction in the decline of forced vital capacity (FVC) over a 12-month period. While pirfenidone was associated with a reduced risk of disease progression or death, its impact on symptoms such as dyspnea and overall mortality was limited. (23)

Nintedanib (Ofev®), by contrast, a tyrosine kinase inhibitor with antifibrotic properties, was approved for the treatment of IPF by the European Medicines Agency (EMA) in January 2015. The following year was commercially available in all European country (24).

Nintedanib is a small molecule indolinone derivative that functions as a potent intracellular tyrosine kinase inhibitor. In IPF, it targets several key pro-fibrotic and pro-angiogenic signalling pathways implicated in disease progression. Specifically, nintedanib inhibits multiple receptor tyrosine kinases, including fibroblast growth factor receptors (FGFR-1, -2, -3), vascular endothelial growth factor receptors (VEGFR-1, -2, -3), platelet-derived growth factor receptors (PDGFR-α and -β), colony-stimulating factor 1 receptor (CSF1R), and FMS-like tyrosine kinase 3 (FLT3) (25) (26) (27).

By competitively binding to the ATP-binding site of these receptors, nintedanib prevents autophosphorylation and disrupts downstream signalling cascades essential for fibroblast activation and proliferation (28).

In addition to receptor inhibition, nintedanib also targets non-receptor tyrosine kinases such as Src and Lck, which further contributes to the suppression of fibrogenic processes (29). Through these combined mechanisms, nintedanib inhibits fibroblast proliferation, migration, and extracellular matrix production—hallmarks of IPF pathology. Furthermore, by attenuating aberrant angiogenesis and tissue remodelling in the lung, nintedanib helps to slow fibrotic progression and may reduce complications such as pulmonary hypertension (27) (30) (31). Fig. 2

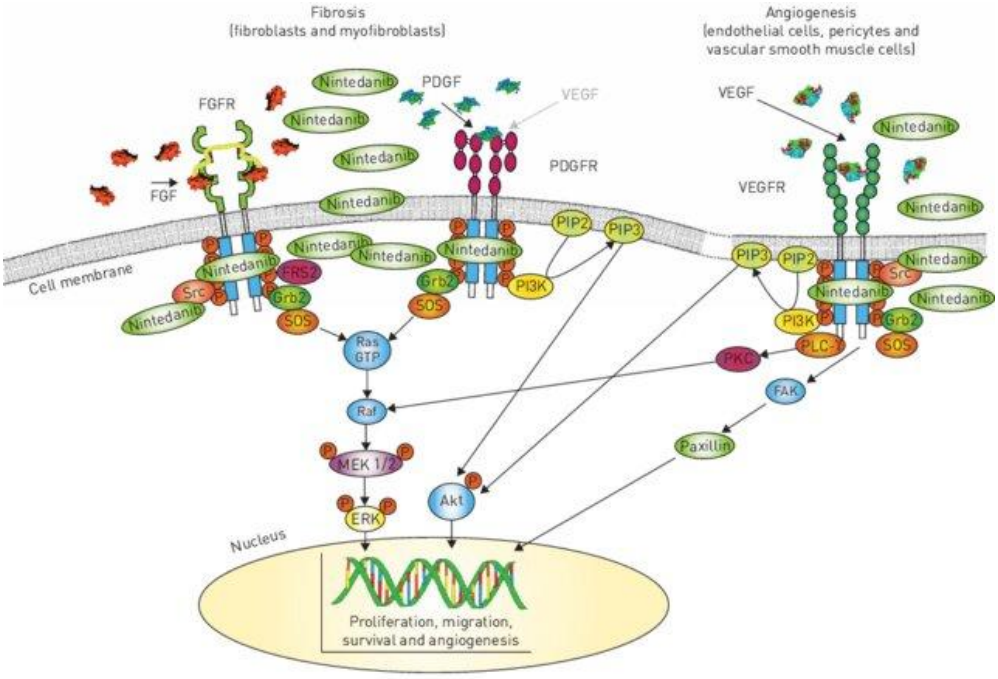

Fig.2 **Mechanism of action of Nintedanib**. Nintedanib inhibits key receptors—FGFRs, PDGFRs, and VEGFRs—by blocking their ATP binding sites, preventing receptor activation and downstream signalling. It also may block non-receptor kinases like Src and Lck. This inhibition reduces fibroblast growth, migration, and survival, and may also limit blood vessel formation in the lungs.

Although nintedanib and pirfenidone represented major therapeutic advances as the first antifibrotic agents approved for IPF, their efficacy remains partial rather than curative. Both drugs slow the rate of FVC decline and may improve progression-free survival. Despite their benefits, both agents act predominantly on downstream fibrotic cascades and fail to address upstream pathogenic drivers such as alveolar epithelial cell senescence, mitochondrial dysfunction, oxidative stress, and aberrant immune activation, which perpetuate fibroblast proliferation and extracellular matrix remodelling.

Over the past decade, more than 25 investigational compounds targeting diverse molecular pathways—including tyrosine kinase inhibitors, anti-TGF-β agents, autotaxin inhibitors, and integrin antagonists—have failed to demonstrate significant clinical benefit or safety advantages in phase II and III trials (32) Fig. 3. These failures underscore the biological complexity and redundancy of fibrogenic signalling in IPF, where multiple interconnected networks involving epithelial–mesenchymal transition, mitochondrial homeostasis, oxidative stress, and immune–fibroblast crosstalk compensate for single-

target inhibition (33) (34).

Molecule	Mechanism of action	Target
Anlotinib	Inhibiting kinases	EMT /Fibroblasts
Treprostinil	Prostacyclin receptor agonist	Fibroblasts
BI 1015550	PDE-4B inhibitor	Fibroblasts
LTI-03	Inhibiting ECM production	MAPK/ERK/ Fibroblasts
BMS-986278	LPA1 antagonist	Fibroblasts
HZN-825	LPAR1 antagonist	Fibroblasts
XFB-19	Inhibiting C/EBPβ	Myofibroblasts
ARO-MMP7	RNA interference	ECM production
Venetoclax	Inhibiting Bcl-2	Macrophages
HuL001	Anti-ENO1 mAb	ECM remodeling
Sufenidone	Inhibiting TGF-β1	TGF-β
Deupirfenidone	Inhibiting TGF-β1	TGF-β
Yifenidone	Inhibiting TGF-β1	TGF-β
SRN-001	RNA interference	TGF-β
Bexotegrast	Inhibiting integrins	TGF-β
Artesunate	Downregulating TGF-β1	TGF-β
Vixarelimab	Anti-OSMR mAb	IL-31/OSM
Axatilimab	Anti- CSF-1R mAb	Macrophages
Atezolizumab	Anti-PD-L1 mAb	Smad3 / β-catenin
Umbilical cord derived MSCs	Immunomodulation, anti-fibrosis and tissue regeneration	Regenerative properties
Lung Spheroid Stem Cells		
Placental MSCs		
Saracatinib	Inhibiting Src kinase	Myofibroblast
TTI-101	Inhibiting STAT3	JAK/STAT pathway
Jaktinib Hydrochloride	Inhibiting JAK1/2	JAK/STAT pathway

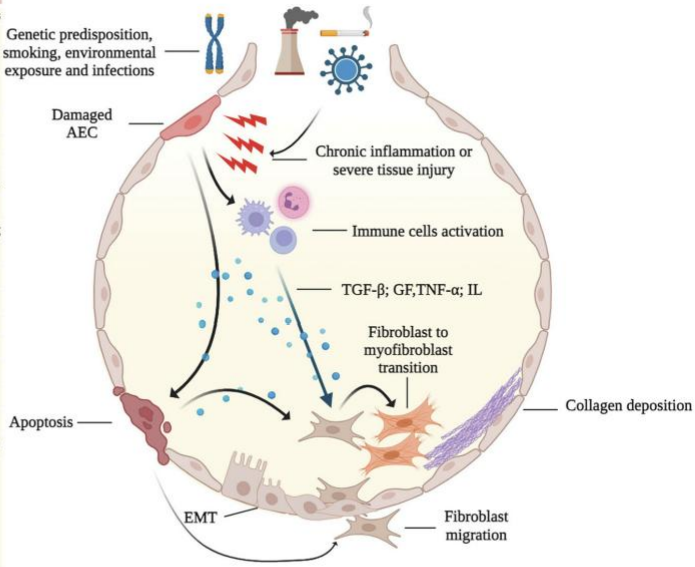

Fig.3 **Schematic Summary of IPF Pathways and Therapeutic Targets**. A schematic representation summarizing the principal molecular pathways implicated in idiopathic pulmonary fibrosis (IPF) and the investigational compounds targeting these mechanisms (34).

This rate underscores the complex, multifactorial nature of IPF, where redundant fibrotic and inflammatory signalling pathways reduce the impact of single-target interventions. Consequently, after ten years of intensive research, nerandomilast (BI 1015550) emerged as the only new therapy to achieve regulatory approval (35) owing to its dual antifibrotic and immunomodulatory mechanisms that address both fibroblast activation and inflammatory signalling, marking a pivotal but incremental step forward in IPF management.

Nerandomilast (BI 1015550) is an orally administered, preferential phosphodiesterase-4B (PDE4B) inhibitor with both antifibrotic and immunomodulatory properties. By selectively inhibiting PDE4B, nerandomilast increases intracellular cyclic adenosine monophosphate (cAMP) levels, leading to downregulation of pro-fibrotic growth factors and inflammatory mediators such as TGF-β and mitogen-activated protein kinase (MAPK) pathways, which are central to the pathogenesis of IPF (36). Clinical studies have demonstrated that nerandomilast slows the rate of lung function decline and may be

used as monotherapy or in combination with existing antifibrotic agents such as nintedanib or pirfenidone. Reflecting its demonstrated efficacy and favorable safety profile, the U.S. Food and Drug Administration approved nerandomilast in October 2025 for the treatment of IPF (35)

1.6 Pathogenetic Models in Idiopathic Pulmonary Fibrosis: Current Concepts

The pathogenesis of IPF is characterized by a complex interplay among genetic, environmental, and cellular factors, ultimately leading to aberrant tissue remodelling and progressive fibrosis. Historically, IPF was thought to be primarily inflammatory in origin, a view supported by the presence of inflammatory cells in bronchoalveolar lavage fluid (37) . However, this perspective has been largely replaced by a more nuanced understanding that centers on repeated or sustained micro-injuries to the alveolar epithelium—particularly type I alveolar epithelial cells (AEC1s)—as the initiating events in a maladaptive repair cascade.

An early and consistent feature of pulmonary fibrosis in humans is a phenotypic change in alveolar epithelial cells (AECs), suggesting that epithelial injury is a critical early event in disease initiation (38) . Although the exact nature of this injury remains uncertain, it is widely believed that the fibroproliferative response is driven by a combination of host-specific susceptibility, genetic predisposition, and environmental exposures. This leads to impaired epithelial regeneration, dysregulated signalling, and persistent activation of fibrotic pathways (39).

A hallmark histopathological feature of usual interstitial pneumonia (UIP), the characteristic pattern of IPF, is the presence of fibroblastic foci. These are localized aggregates of myofibroblasts, which are the key effector cells in fibrosis and underlie areas of damaged or altered epithelium (40). Recent evidence suggests that fibroblastic foci may form an interconnected network rather than originating from isolated sites of injury, indicating a more systemic or diffuse pathological process (41).

Persistent or repetitive injury appears to provoke a dysregulated wound healing response,

characterized by defective alveolar re-epithelialization, unchecked myofibroblast proliferation, and excessive extracellular matrix (ECM) deposition within the pulmonary interstitium. These pathological changes lead to progressive scarring and loss of functional lung architecture (42).

Current prevailing hypotheses emphasize the disrupted crosstalk between epithelial and mesenchymal cells as a central mechanism in IPF pathogenesis. This impaired communication may be further exacerbated by immune-mediated responses, adding another layer of complexity to the disease process.

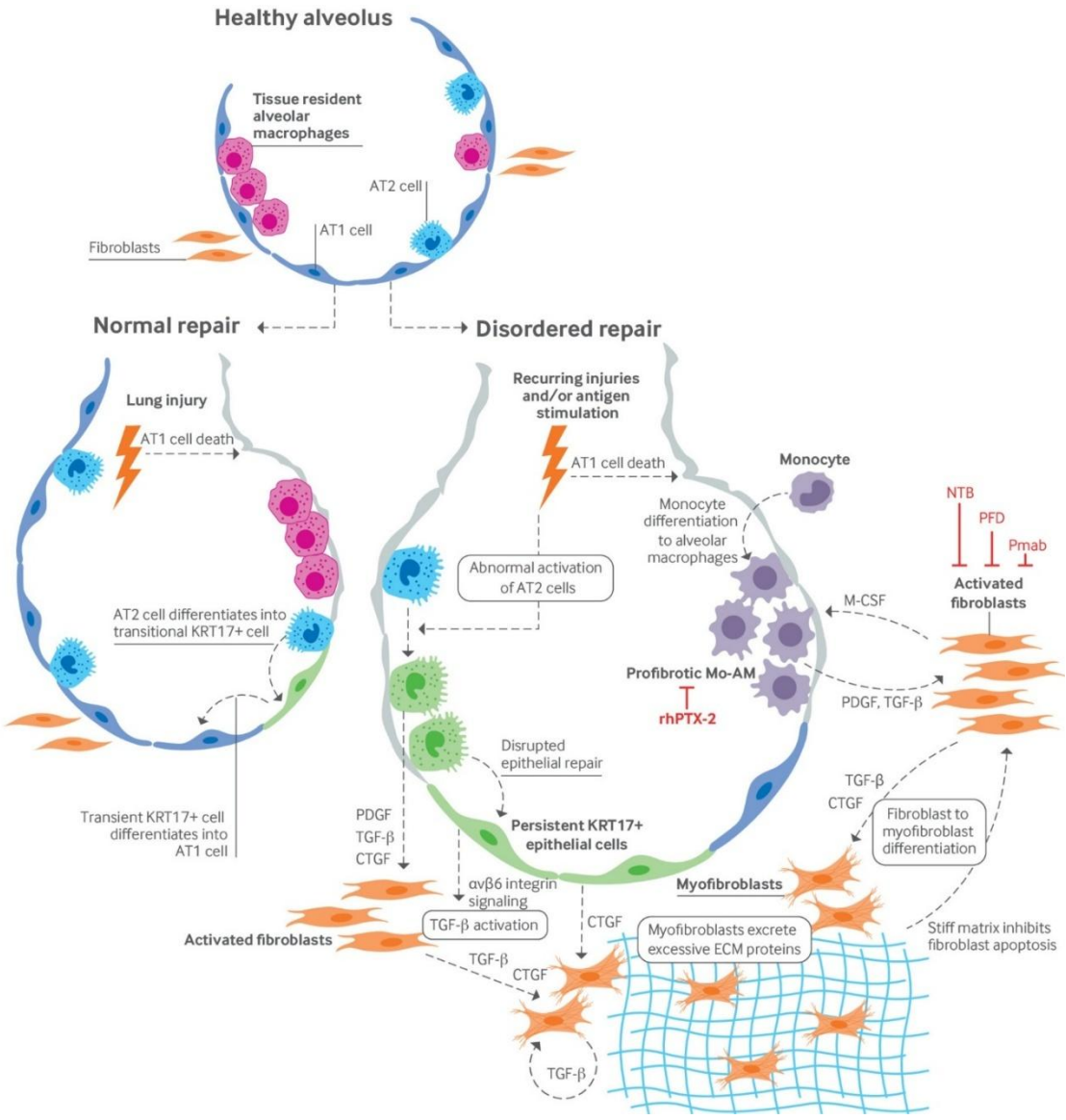

Fig.4 Mechanisms and signals involved in the development of pulmonary fibrosis and therapeutic targets. (43)

1.7 Insights into the Underlying Mechanisms of Idiopathic Pulmonary Fibrosis

Currently hypotheses propose that IPF arises as a result of a highly aberrant wound healing response in susceptible individuals following repetitive or persistent epithelial injury. Mechanistic insights into IPF have delineated a triphasic model of disease development: **(1) Predisposition**, involving genetic susceptibility (e.g., polymorphisms in TNF, IL-1 receptor antagonist, and surfactant protein genes), aging, and environmental exposures (e.g., organic/inorganic dusts, solvents); **(2) Initiation**, characterized by alveolar epithelial injury, activation of profibrotic mediators such as TGF-β, epithelial-to-mesenchymal transition (EMT), recruitment of circulating fibrocytes, and induction of the unfolded protein response (UPR); and **(3) Progression**, marked by persistent fibroblast activation, differentiation into myofibroblasts, extracellular matrix (ECM) deposition, and mechanical remodelling of the pulmonary interstitium (44).

Environmental insults, whether infectious (e.g., Epstein-Barr virus, HCV, influenza A) or non-infectious (e.g., particulate matter, metal dust, wood dust), exacerbate epithelial injury and facilitate AEC2 hyperplasia. Although AEC2s typically contribute to epithelial regeneration by differentiating into AEC1s, in IPF, this process is dysregulated. Under persistent profibrotic signalling, particularly via TGF-β, AEC2s undergo hyperplastic expansion without appropriate differentiation, resulting in alveolar collapse and impaired gas exchange. Additionally, TGF-β and other mediators such as PDGF, IGF-1, and endothelin-1 stimulate fibroblast proliferation and transformation into myofibroblasts. Fig. 5 (45).

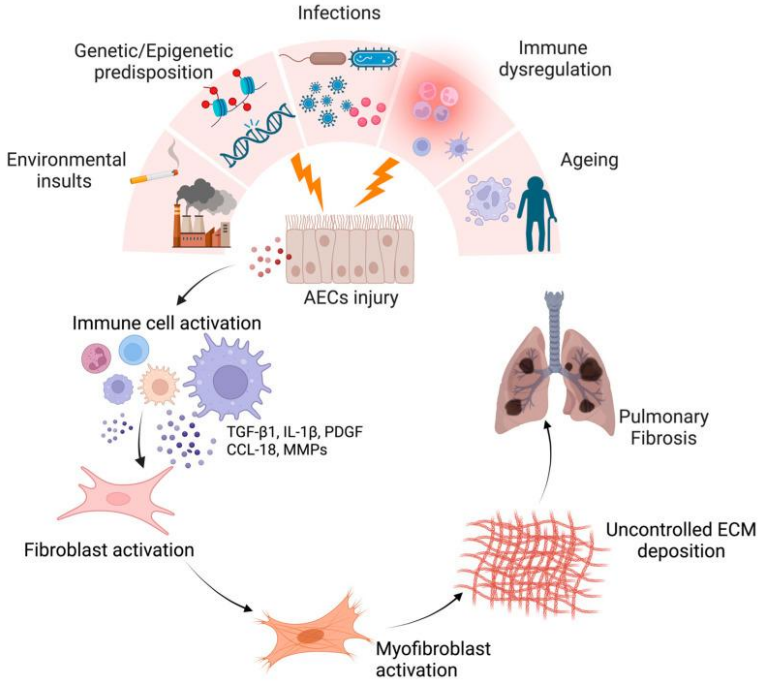

Fig.5 **Pathophysiological Cascade Leading to Pulmonary Fibrosis**. Repetitive epithelial injury triggers dysregulated repair responses in the lung. Damaged alveolar epithelial cells release inflammatory and fibrotic mediators that recruit immune cells and activate fibroblasts. Persistent activation leads to excessive myofibroblast differentiation and extracellular matrix deposition, causing scarring, impaired gas exchange, and progressive respiratory decline. (45)

The process of EMT is central to the fibrotic response. Following epithelial injury, cells lose polarity, downregulate epithelial markers (e.g., E-cadherin), and upregulate mesenchymal markers (e.g., N-cadherin, fibronectin), acquiring migratory and invasive properties. Several injurious stimuli—including TGF-β1, oxidative stress, Fas activation, and angiotensin II—contribute to EMT and activate fibroblasts to secrete excessive ECM components, particularly type I and III collagens. TGF-β3, released in response to cytoskeletal stress through αvβ6 integrin and UPR activation, is a potent inducer of apoptosis and fibroblast-to-myofibroblast transition. Myofibroblasts, predominantly located in fibroblastic foci, are resistant to apoptosis and are the principal source of ECM proteins including fibronectin, tenascin, proteoglycans, and collagens (46).

The ECM in IPF is not a passive scaffold but a bioactive matrix that regulates cellular behaviour via mechanotransduction and biochemical signalling. It influences

transcriptional and translational activity in fibroblasts, modulating the expression of genes such as COL1A1, COL1A2, COL3A1, COL5A2, COL4A2, and MMPs (e.g., MMP2, MMP3, MMP10), as well as tissue inhibitors of metalloproteinases (e.g., TIMP2). Dysregulated ECM homeostasis results in desmoplasia, characterized by excessive fibril crosslinking, increased matrix stiffness, and an imbalance between ECM synthesis and degradation. Damaged epithelial, endothelial, and smooth muscle cells release proinflammatory and profibrotic mediators—including IL-1, IL-6, IL-13, IL-33, TNF-α, FGF, and leukotrienes—that promote further fibroblast activation, ECM production, and immune cell recruitment, establishing a positive feedback loop of chronic tissue remodelling (47).

A key component of the fibrotic process is the mechanical feedback between cells and the ECM. Fibroblasts and myofibroblasts sense and respond to mechanical cues via actin–myosin contractility and focal adhesion complexes. This mechanotransduction not only supports cell survival and matrix deposition but also contributes to further stiffening of the lung parenchyma, thereby perpetuating fibrosis. (48)

IPF pathogenesis reflects a convergence of epithelial dysfunction, fibroblast activation, immune dysregulation, and matrix remodelling (49). Chronic injury leads to sustained activation of profibrotic pathways and aberrant repair mechanisms that result in irreversible architectural distortion and functional decline of the lung. Understanding these interrelated molecular and biomechanical pathways is essential for developing targeted antifibrotic therapies. Fig. 6

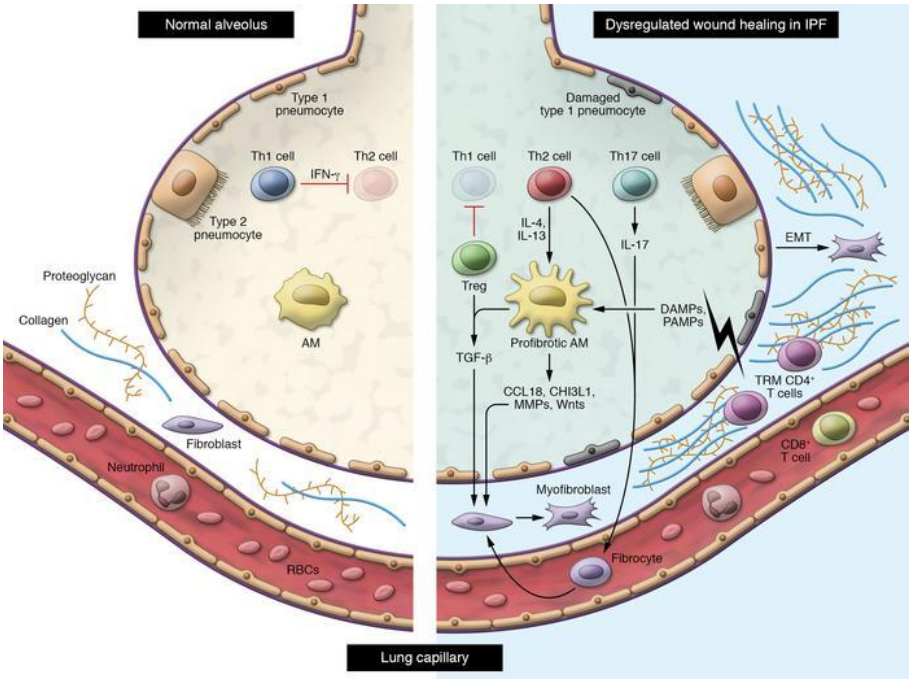

Fig. 6 **Role for immune dysregulation in promoting the development of pulmonary fibrosis.** Profibrotic responses are driven by M2 macrophages, Th17 cells, CD8+ T cells, and potentially Tregs, whereas Th1 cells and TRM CD4+ T cells may play a protective role against fibrosis (49).

CHAPTER 2: The role of immunity in the pathogenesis of IPF

2.1 General immunology of lung

The lung occupies a unique position between the host and the external environment with the alveolar space being separated from the vasculature by a barrier of only 4–8 μm, the alveolar-capillary membrane (ACM) (50). As the lungs are in direct contact with the surrounding environment, this requiring a tightly regulated balance between immune defence and preservation of gas exchange. To meet this challenge, the pulmonary immune system is composed of both innate and adaptive components, operating in tandem to balance host defence with the need to preserve lung structures. (51)

Innate immune mechanisms, the first line of defence, rapidly responding to pathogens and inhaled particulates through phagocytosis and the release of pro-inflammatory

cytokines. Adaptive immunity, mediated by $CD4^+$ and $CD8^+$ T lymphocytes, provides antigen-specific responses and immunological memory. (52)

2.2 Innate immunity in IPF

The interplay of Innate immune cells, including macrophages, neutrophils, fibrocytes, myeloid-derived suppressor cells (MDSCs), and innate lymphoid cells (ILCs), drives the chronic inflammation and tissue remodelling. The main roles of these cells in IPF are described in Table 2.

Table 2. Role of innate immune cells in IPF

Innate immune cells	Role in IPF	Reference
Neutrophil	Neutrophil extracellular traps (NETs) are implicated in fibrotic processes.	(53) (54) (55)
Macrophages	M1 macrophages exhibit pro-inflammatory and anti-fibrotic functions, whereas M2 macrophages are associated with anti-inflammatory, pro-fibrotic, and tissue-regenerative roles.	(56) (57)
Monocytes	Serve as precursors for pro-fibrotic macrophages and fibrocytes. Secrete inflammatory cytokines that promote fibrosis. Elevated monocyte counts correlate with worse survival outcomes.	(58) (59)
	Contribute to fibroblast-driven tissue	

Fibrocytes	remodelling and fibrosis in the lung.	(60)
Myeloid-derived suppressor cells (MDSCs)	Increased MDSC levels correlate with reduced lung function, severe pulmonary hypertension, and elevated regulatory T cell counts. These cells play a role in pro-fibrotic and immune-dysregulated environments.	(60) (61)
Type-2 innate lymphoid cells (ILC2s)	An increase in ILC2s in IPF patients' BAL fluid is linked to a heightened type-2 immune response. ILC2s promote extracellular matrix (ECM) synthesis and tissue remodelling through IL-13 production.	(62) (63)
Dendritic cells (DCs)	Accumulation of immature DCs occurs in areas of epithelial hyperplasia and fibrotic lesions. Mature DCs localize in lymphoid follicles, where they interact with T and B cells, potentially sustaining ongoing inflammation in the lungs.	(64) (65)

2.2.1 Natural Killer cells in IPF

NK cells are cytotoxic lymphocytes that play a crucial role in the innate immune system by eliminating infected, tumorigenic, or senescent cells. Two major NK cell subsets have been identified: circulating cytotoxic NK cells ($CD56^{dim}CD16^{+}$, or ci-NK) and tissue-resident proinflammatory NK cells ($CD56^{bright}CD16^{-}$, or tr-NK). Recent findings indicate a significant reduction in both the number and activity of lung-resident NK cells in the lung tissue and BAL of IPF patients, (66) (67) (68). Conversely, an increased proportion of ci-NK cells in the PBMC of IPF patients suggests impaired NK cell trafficking or recruitment into the lung(69). Furthermore, these NK cells exhibit markers of immunosenescence (metallothionein enzymes, zinc metabolism enzymes) and reduced cytotoxic function, which may hinder the clearance of senescent cells known to accumulate and contribute to fibrosis through the senescence-associated secretory phenotype (SASP) (67). Further mechanistic evidence indicates that chronic inflammatory and oxidative stress conditions in the fibrotic lung can reprogram NK cell metabolism, leading to altered mitochondrial function, increased expression of inhibitory receptors, and impaired production of key effector molecules such as perforin and granzyme B (70). Such metabolic exhaustion parallels phenotypes observed in other chronic inflammatory disorders, reinforcing the notion that NK cell dysfunction in IPF reflects both senescence-associated and metabolic defects. Dysfunctional NK cell responses—marked by impaired recruitment, metabolic reprogramming, and loss of cytotoxicity—create a permissive immune milieu that fosters fibrotic remodelling and disease progression in IPF (71).

2.3 Adaptive immunity in IPF

The role of T lymphocytes in the pathogenesis of IPF remains a subject of ongoing investigation, yet a growing body of evidence implicates these adaptive immune cells in both the initiation and progression of disease (59). These T cells are often localized to fibrotic regions, displaying variable distributions ranging from diffuse alveolar and interstitial infiltration to organized perivascular aggregates and tertiary lymphoid follicles (72). Experimental models and transcriptomic studies highlight the dualistic nature of T cells in fibrosis, with subsets exhibiting either profibrotic or antifibrotic roles depending

on their cytokine profiles and activation states. $CD4^+$ T cells mediate immune regulation through secretion of cytokines such as IL-4, IL-13, IFN-γ, and TGF-β, while $CD8^+$ T cells contribute primarily through cytotoxic mechanisms (73). These findings collectively suggest that T lymphocytes, particularly activated $CD4^+$ memory cells, are not merely bystanders but active participants in the immunopathogenesis of IPF—potentially through antigen-specific responses, chronic immune activation, and aberrant epithelial–mesenchymal interactions (74).

2.4 $CD4^+$ T lymphocytes in IPF

$CD4^+$ T lymphocytes play a central role in orchestrating adaptive immune response involved in the pathogenesis of IPF. These cells are often abundant found in fibrotic region compared to areas of preserved lung architecture, and their abundance has been associated with poorer lung function and reduced survival. $CD4^+$ T cells in IPF display signs of chronic activation, including elevated surface expression of MHC class II and CD40L, and exhibit a memory phenotype ($CD45RO^+$), indicating previous antigen exposure (75). Moreover, clonal expansions of T cell receptor beta chain variable (TCRBV) regions suggest oligoclonal proliferation driven by antigenic stimulation (76). Within the IPF lung, $CD4^+$ T cells frequently localize to tertiary lymphoid structures—ectopic lymphoid aggregates resembling germinal centers—where they may contribute to lymphoid neogenesis, ongoing immune activation, and fibroblast modulation (72). These findings collectively suggest that activated $CD4^+$ memory cells, are not merely bystanders but active participants in the immunopathogenesis of IPF—potentially through antigen-specific responses, chronic immune activation, and aberrant epithelial–mesenchymal interactions (74). Depending on their functional polarization and cytokines release, $CD4^+$ helper cells can be classified as T helper type 1 (Th1) cells, T helper type 2 (Th2) cells, T helper type 17 (Th17), regulatory T cells (Treg). Fig.7

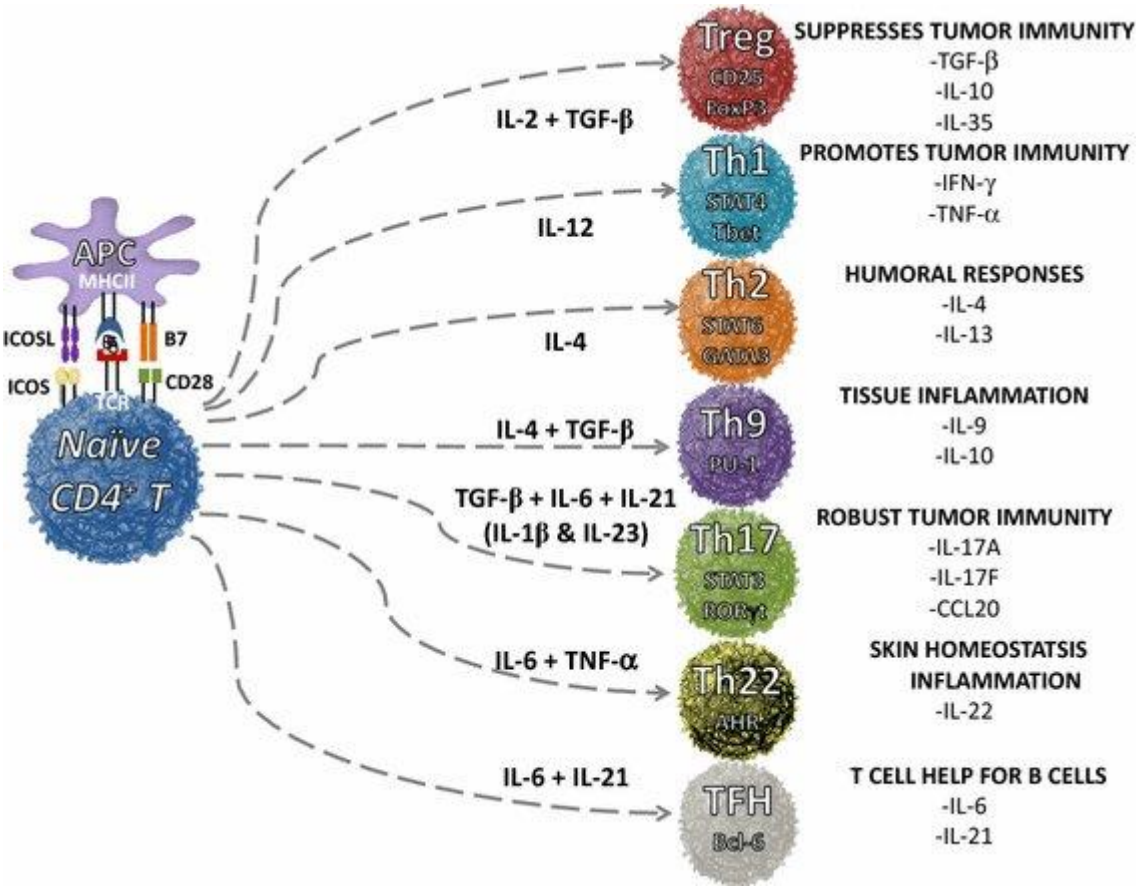

Fig.7 **Differentiation of helper T cell subsets from naive CD4⁺ T cells mediated by cytokines and co-signals.** Various cytokines and co-stimulatory signals from antigen-presenting cells drive the differentiation of distinct T cell subsets, including Th1, Th2, Th17, Th9, Th22, Tfh, and Treg cells. These subsets, regulated by key transcription factors such as T-bet, GATA3, RORγt, STATs, and FoxP3, coordinate immune responses to pathogens, self-antigens, and tumours. (77)

2.4.1 T helper cell subsets

Th1 cells and their secretory products are considered anti-fibrotic. They release IL-2, IFN-γ, TNF, IL-12, and IL-18. IFN-γ is typically antifibrotic because it suppresses collagen deposition by fibroblasts. Thus, Th1 cells, which are derived from Th0 cells that are activated by IL-12, are widely recognized as antifibrotic T cells due to their production of IFN-γ (78). In contrast, Th2 cells are generally associated with pro-fibrotic effects in IPF. These cells produce IL-4, IL-5, and IL-13, which promote fibroblast proliferation and differentiation into myofibroblasts, driving the fibrotic process. Elevated levels of

Th2 cytokines, particularly IL-4 and IL-13, have been detected in the BAL fluid of IPF patients, confirming their role in fibrosis. Moreover, IL-4 has been shown to protect myofibroblasts from apoptosis, thereby fostering the persistence of fibrosis (79) (59). It has been suggested that an imbalance of Th1/Th2 when there is an overactive pro-fibrotic Th2 response and an underactive anti-fibrotic Th1 response contribute to the process of pulmonary fibrosis (80).

Th17 cells represent another important subset in IPF. Studies demonstrate that they are profibrotic due to the typically characteristic to produce IL-17, elevated expressed on BAL fluid of IPF patients (81). Moreover, the IL-17 receptor that respond to IL-17 is expressed in lung fibroblast of BAL fluid of IPF patients lead to production of ECM and proliferation (82), often in association with with TGF-β signalling (81). Furthermore, the ability of IL-17A to recruit neutrophils to the site of fibrosis highlights its critical role in disease progression (73). Tregs have a dual role in IPF, with their function being highly dependent on the disease stage. They are generally considered anti-fibrotic due to their production of IL-10 and TGF-β, which regulate immune responses and maintain tissue homeostasis. However, their role in fibrosis is context-dependent. Early in the disease, Tregs may promote fibrosis by producing TGF-β1, a pro-fibrotic factor**,** and facilitating collagen deposition (83). This duality is exemplified by Sema7a+CD4+CD25+FoxP3+ Treg subsets, which can enhance TGF-β1-mediated fibrosis (84). In contrast, depletion of Tregs early in the disease can reduce lung inflammation and collagen deposition, suggesting their protective role in later stages. Moreover, an imbalance between Treg and Th17 populations, as seen in IPF, contributes to disease progression. These findings underscore the complexity of Treg function in fibrosis and suggest that their modulation could potentially alter the disease course.

2.5 $CD8^+$ T lymphocytes in IPF

Cytotoxic T lymphocytes (CTLs), identified by CD8 expression, are integral to the adaptive immune response and are traditionally recognized for their roles to contrast intracellular pathogens and malignant cells through the secretion of interferon-γ (IFN-γ) and cytotoxic granules such as granzyme B and perforin. Recent evidence suggests that

$CD8^+$ T cells may also contribute significantly to the pathogenesis of IPF. Single-cell RNA sequencing and immunophenotyping of lung tissue and bronchoalveolar lavage fluid from IPF patients have revealed an increase expression of $CD8^+$ T cells, which correlate with greater fibrotic burden and reduced lung function, including decreased of DLCO, increasing shortness of breath and worse gas exchange (85). The presence of CD8+ T lymphocytes, especially in response to persistent viral infections such as Epstein-Barr Virus, influenza, and cytomegalovirus, supports the hypothesis that an excessive or chronic activation of CD8+ T cells could contribute to the development of lung damage and fibrosis. Experimental studies have shown that CD8+ T cells, upon recognition of an alveolar epithelial autoantigen, can trigger inflammatory cascades that lead to interstitial pneumonia and fibrotic changes. Furthermor data support a model in which $CD8^+$ T cells — and in particular tissue-resident, granzyme$^+$ memory subsets — contribute to fibrotic lung remodelling via chronic cytotoxic/inflammatory activity, and that CCL18/CCR8 signalling is one mechanistic link (86). These cells are also retained in the lung via CXCR6 and CD103-mediated interactions, and their presence has been linked to ongoing inflammation and tissue remodelling (85) (87).

CD8 T cells can differentiate into subtypes, such as Tc1 cells (producing IFN-γ) and Tc2 cells (producing IL-4), based on cytokine release, each with distinct roles in fibrosis. Tc1 cells, which produce IFN-γ but not IL-4, are thought to attenuate fibrosis, whereas Tc2 cells, which produce IL-4 but not IFN-γ, have been linked to the promotion of fibrosis. Study showed that in bleomycin (BLM)-induced mouse models of pulmonary fibrosis, $CD8^+$ T cell was significantly increased compared to controls (88).

$CD8^+$ T cells in fibrotic lungs exhibit features of chronic activation and exhaustion, marked by elevated expression of immune checkpoint molecules such as PD-1 and PD-L1, indicating persistent antigenic stimulation within a profibrotic microenvironment. Additionally, it was demonstrated that a depletion and modulation of $CD8^+$ T cells using neutralizing antibodies and through vitamin D_3 supplementation, attenuate fibrosis in animal models by enhancing their cytotoxic efficiency and restoring immune homeostasis (86) (89). These findings suggest that exhausted phenotypes of $CD8^+$ T cells and resident memory subsets, contribute to chronic inflammation and persistence of a fibrogenic microenvironment in IPF.

2.6 Immune checkpoint: PD-1

Immune checkpoints are protein mainly expressed on cell surfaces that help maintain self-tolerance and prevent autoimmune diseases. They are expressed on -antigen presenting cells (APCs), such as dendritic cells (DCs), that engage specific receptor partners expressed by T lymphocytes and either drive their activation and differentiation (positive immune checkpoint molecules) or promote immunoregulatory effects (negative immune checkpoint molecules) (90) .

Programmed cell death-1 (PD-1) is a type I transmembrane receptor belonging to the immunoglobulin superfamily, characterized by a cytoplasmic domain containing two inhibitory motifs: an immunoreceptor tyrosine-based inhibition motif (ITIM) and an immunoreceptor tyrosine-based switch motif (ITSM) (91) . Fig. 8

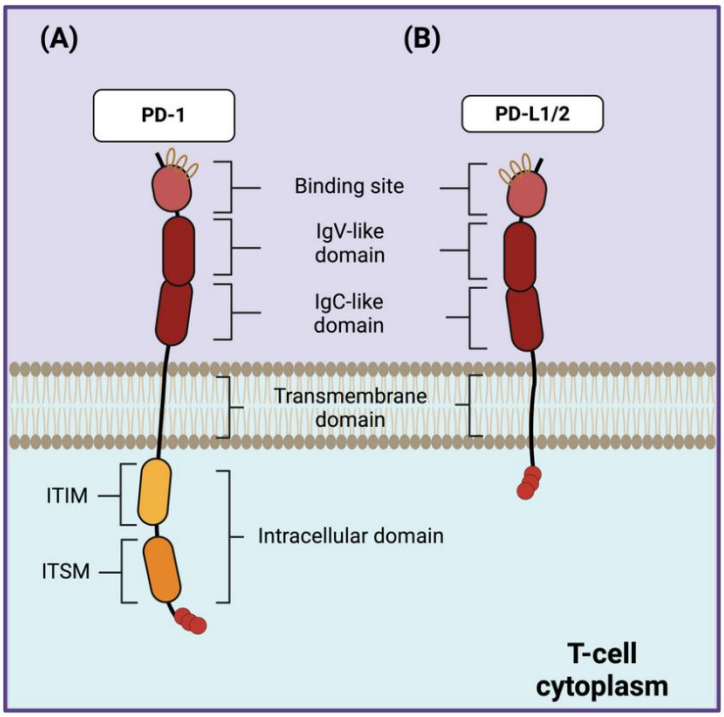

Fig.8 **Structure of PD-1 and its ligands PD-L1/2.** (A) PD-1 consists of two extracellular immunoglobulin-like domains (IgV and IgC), a transmembrane segment, and an intracellular tail containing ITIM and ITSM signalling motifs. (B) Its ligands, PD-L1 and PD-L2, share a similar extracellular immunoglobulin-like structure (91).

PD-1 is broadly expressed on various immune cells, including activated T cells, B cells, natural killer cells, macrophages, dendritic cells, and monocytes, as well as specific T cell

subsets such as exhausted T cells, regulatory T cells (Tregs), follicular helper T cells, follicular regulatory T cells, and memory T cells (92). Its expression is induced by multiple stimuli, including antigen receptor signalling (via TCR or BCR) (93), cytokines such as IL-2, IL-7, IL-15, and IL-21, infectious agents, and lipopolysaccharide (LPS). The primary ligands for PD-1, programmed death-ligand 1 (PD-L1) and PD-L2, belong to the B7 family; PD-L2 expression is largely restricted to professional antigen-presenting cells (APCs) such as dendritic cells and macrophages, whereas PD-L1 is widely expressed on hematopoietic cells including activated T cells (94). PD-1 and its ligands can interact both in trans between adjacent cells and in cis on the same cell surface, underscoring the complexity of co-stimulatory and co-inhibitory molecular interactions within the immune microenvironment. Upon ligand engagement, PD-1 signalling inhibits T cell receptor (TCR) signalling by suppressing CD3ζ chain phosphorylation and ZAP-70 association, leading to downregulation of the Ras and Bcl-xL pathways that regulate proliferation and survival, respectively. Furthermore, PD-1 signalling upregulates the transcription factor BATF, impairing T cell effector function, and inhibits the phosphatidylinositol 3-kinase (PI3K)/Akt pathway, with downstream effects including mTOR downregulation and increased FoxO1 stability, resulting in altered T cell metabolism characterized by reduced glycolysis and enhanced fatty acid oxidation (95). These mechanisms collectively induce T cell exhaustion, marked by diminished proliferation, effector cytokine production (e.g., TNF-α, IFN-γ, IL-2), and functional impairment. PD-1 signalling is also self-reinforcing through FoxO1-mediated upregulation of PD-1 expression. In the context of IPF, PD-1 has been implicated in several pathogenic mechanisms: overexpression of PD-1 on Th17 cells may enhance STAT3 transcriptional activity via indirect inhibition of PI3K, contributing to the conversion of Tregs into Th17 cells under the influence of elevated IL-6, thereby increasing IL-17 and TGF-β production and promoting fibrosis (96). Moreover, PD-1 expressed on T cells binds PD-L1, which is upregulated on lung fibroblasts, activating signalling pathways including p53, focal adhesion kinase (FAK), Smad3, and β-catenin. PD-L1 upregulation confers apoptosis resistance and phagocytosis evasion to myofibroblasts by inhibiting p53 and activating FAK, promoting excessive myofibroblast proliferation. Additionally, PD-L1 mediates fibroblast-to-myofibroblast transition (FMT) through Smad3 and β-catenin pathways, stimulates extracellular matrix deposition by

inhibiting autophagy, and suppresses adaptive immunity, facilitating immune evasion. The transcription factor JUN further upregulates PD-L1 and CD47 in fibroblasts and dormant macrophages, leading to T cell exhaustion and macrophage quiescence, which collectively enable myofibroblast persistence and resistance to immune clearance. JUN also regulates IL-6 expression at the chromatin level, enhancing immunosuppressive responses characterized by T cell exhaustion and expansion of activated Tregs (97). Thus, the PD-1/PD-L1 axis represents a multifaceted regulator of immune dysfunction and fibrotic remodelling in IPF, balancing immune tolerance and profibrotic signalling pathways that contribute to disease progression (98)

2.6.1 PD-1 in Idiopathic pulmonary fibrosis

Programmed cell death protein 1 (PD-1) functions as a critical immune checkpoint receptor, traditionally recognized for its role in attenuating immune responses and maintaining tolerance. In IPF. PD-1 expression is markedly upregulated on $CD4^+$ T cells, particularly within the T helper 17 (Th17) subset, implicating PD-1 as a key modulator of fibrotic pathogenesis. Elevated PD-1 on Th17 cells has been shown to enhance signal transducer and activator of transcription 3 (STAT3) activity, a pivotal transcription factor promoting the production of interleukin-17A (IL-17A) and TGF-β. Mechanistically, PD-1 may indirectly increase STAT3 activation through the inhibition of phosphatidylinositol 3-kinase (PI3K), thus relieving the negative regulation of STAT3 and amplifying fibrogenic signalling pathways. This PD-1–mediated modulation of Th17 cells contributes to the expansion of profibrotic cytokine milieu, driving fibroblast activation and extracellular matrix deposition (96). Furthermore, PD-1 expression promotes the plasticity of regulatory T cells (Tregs), facilitating their conversion into Th17-like cells under the influence of elevated IL-6, thereby compounding the profibrotic and proinflammatory environment. Beyond T cells, PD-1 interactions with its ligand PD-L1 on lung fibroblasts have been implicated in enhancing fibrosis by promoting fibroblast resistance to apoptosis and phagocytosis, although this primarily involves the PD-L1 axis (98) .

Collectively, these findings position PD-1 not only as a critical checkpoint receptor

governing immune exhaustion but also as an active participant in the pathogenic signalling cascades underlying IPF progression, underscoring its potential as a therapeutic target to mitigate fibrotic lung disease (99). Fig. 9

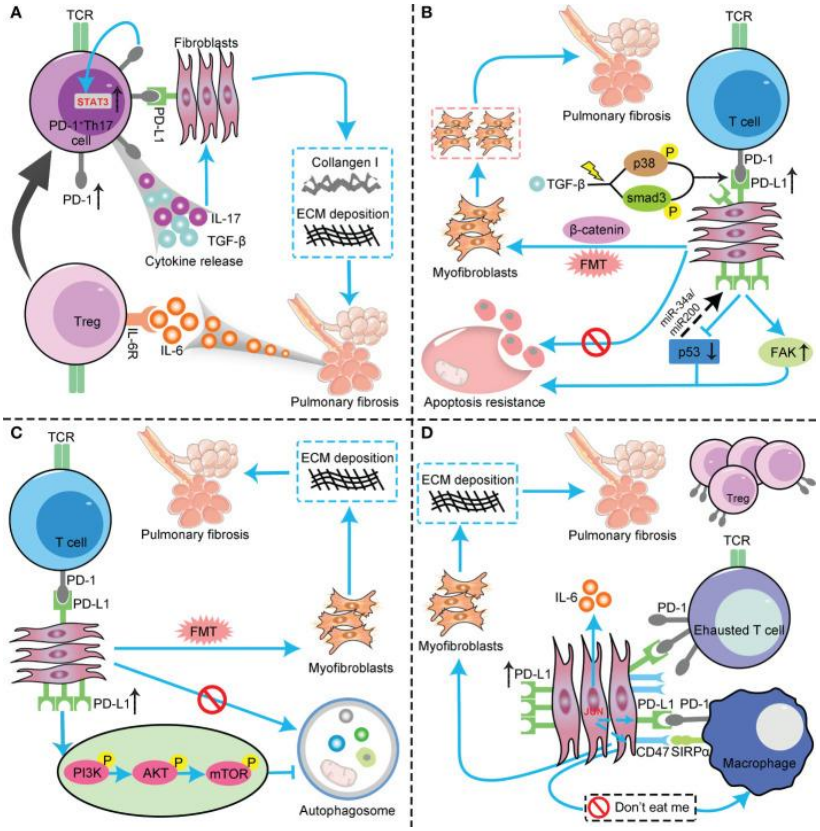

Fig. 9 **The PD-1/PD-L1 axis as a driver of fibrotic remodelling in IPF through multifaceted intercellular and signalling interactions.** The PD-1/PD-L1 axis contributes to idiopathic pulmonary fibrosis (IPF) by promoting profibrotic signalling across multiple cell types. PD-L1 upregulation enhances Th17-mediated IL-17 and TGF-β production, activates fibroblast survival and differentiation via p53, FAK, Smad3, and β-catenin pathways, and suppresses autophagy and adaptive immunity. These effects collectively drive myofibroblast proliferation, extracellular matrix accumulation, and immune evasion, leading to progressive fibrosis. (96)

CHAPTER 3

3.1 Hypothesis

In this research project, we hypothesize that patients with IPF exhibit systemic immune alterations characterized by an imbalance within the T-cell compartment. We postulated that $CD8^+$ T cells from IPF patients display an altered functional phenotype compared with those from healthy individuals, with evidence of chronic activation, impaired cytotoxicity, and features of exhaustion. We also hypothesize that pharmacological modulation with the antifibrotic agent nintedanib and/or immune checkpoint inhibition through anti-PD1 therapy can differentially regulate the activation state and effector functions of $CD8^+$ T cells, potentially restoring aspects of immune balance and contributing to the understanding of immunoregulatory mechanisms in IPF pathogenesis.

3.2 Aim of the Study

The present study aimed to investigate the immunological landscape of IPF through a combined phenotypic and functional analysis of peripheral immune cells, with particular emphasis on the $CD8^+$ T-cell compartment. Initially, a comprehensive immunophenotypic characterization of peripheral blood mononuclear cells (PBMCs) was performed to assess the expression of inhibitory receptors PD-1 and TIGIT on $CD4^+$, $CD8^+$, and $CD56^+$ cell subsets, to define systemic immune alterations associated with IPF. Subsequently, purified $CD8^+$ T cells from IPF patients and HCs were evaluated under basal and stimulated conditions, including exposure to anti-PD1 antibody, nintedanib, or their combination, to examine the modulation of several functional markers o CD8+ cells which characterized activation (CD69, CD25), exhaustion (PD-1, TIGIT), cytotoxic (Granzyme B, Perforin, LAMP-1), and recruitment(ICAM-1). These experiments were designed to elucidate the effects of immune checkpoint blockade and antifibrotic treatment on $CD8^+$ T-cell function and phenotype.

CHAPTER 4: Material and methods

4.1 Ethical approval

The study was conducted in accordance with the Declaration of Helsinki and approved by the Local Ethics Committee of Siena University Hospital (C.E.A.V.S.E.) (protocol code Markerlung 17431; date of approval 15 June 2020). All patients gave their written informed consent for participation in the study.

4.2 Study population

A total of 52 patients diagnosed with IPF were enrolled in the study. All patients were monitored at the Rare Lung Disease Centre of Siena University Hospital. The diagnosis of IPF was confirmed by a multidisciplinary team, following the international guidelines of the American Thoracic Society/European Respiratory Society (ATS/ERS) (19).

Each patient underwent a comprehensive respiratory evaluation, including lung function tests (LFTs) and high-resolution computed tomography (HRCT) of the chest. All IPF patients were enrolled prior to the initiation of any pharmacological treatment and showed no signs of acute exacerbation or significant disease progression at the time of sampling.

In addition, twelve healthy donors, matched for age and sex, were enrolled as controls. All participants were screened to confirm the absence of autoimmune or vascular diseases.

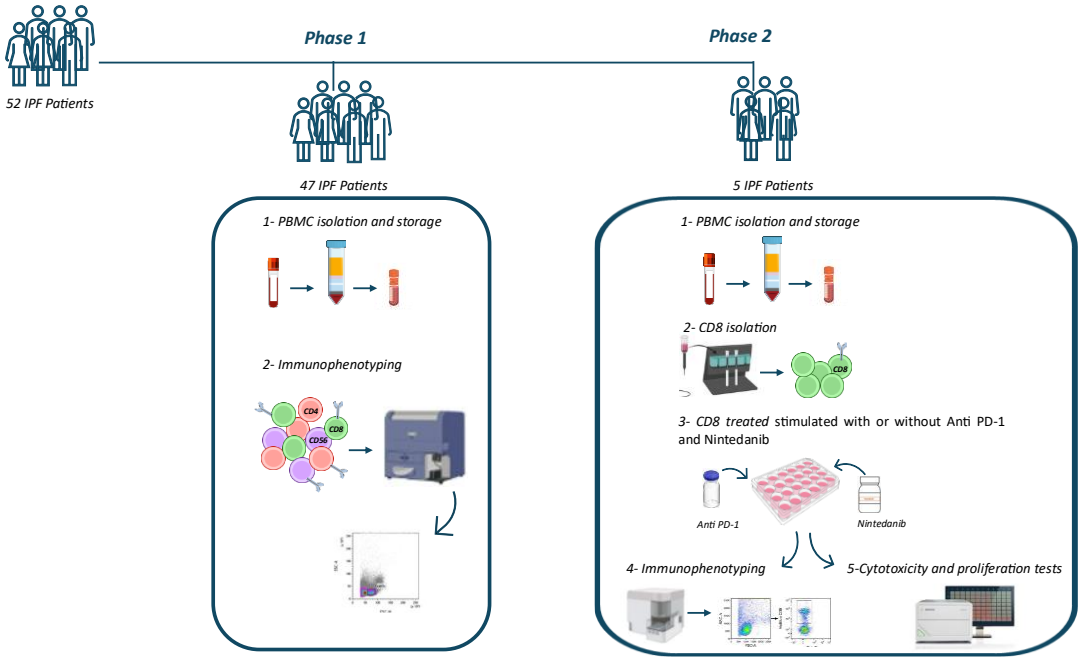

Fig. 10 **Experimental design and workflow of the study**. Phase 1 involved peripheral blood mononuclear cell (PBMC) isolation and immunophenotyping from 47 idiopathic pulmonary fibrosis (IPF) patients. In Phase 2, PBMCs from 5 IPF patients were used for $CD8^+$ T-cell isolation, followed by stimulation with or without anti-PD-1 and nintedanib, and subsequent assessment of immunophenotype, cytotoxicity, and proliferation.

4.3 Peripheral Blood Mononuclear Cells

Peripheral blood mononuclear cells (PBMCs) were collected and handled at the Respiratory Disease Unit laboratory, Siena University Hospital (Italy). Blood samples were drawn into tubes containing EDTA anticoagulant (BD Vacutainer® EDTA tubes, BD Biosciences, CA, USA) and processed within 8 hours. PBMCs were then isolated by density gradient centrifugation using Ficoll Histopaque®-1077 (Sigma-Aldrich, St. Louis, MO, USA) at 1050 × g for 30 minutes without brake, followed by two washes. Cells were resuspended at a concentration of 2 × 10^6 per vial in freezing medium composed of 80% RPMI 1640, 10% fetal bovine serum (FBS), and 10% dimethyl sulfoxide (DMSO, Sigma-Aldrich, St. Louis, MO, USA), then stored in liquid nitrogen until further use. Fig. 11

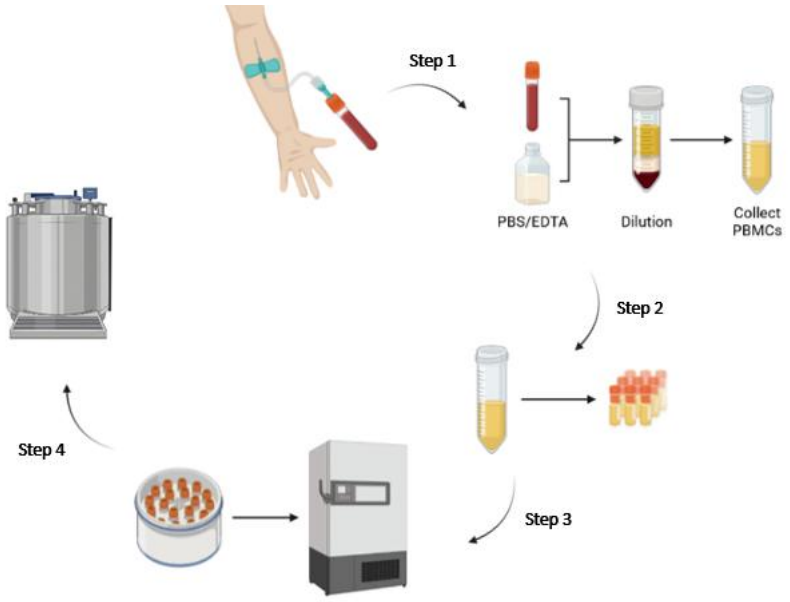

Fig. 11 **Isolation and storage of Human Peripheral Blood Mononuclear Cells (PBMC)**

4.4 Flow Cytometry- Immunophenotyping

Phase 1-Immunophenotyping

Initially, to characterize the general immunophenotype, PBMC from patients with IPF and HCs were stained with a surface panel of antibodies design to characterize major immune cells subsets, including CD4, CD8, CD56 T cells their expression of two immune checkpoints PD-1 and TIGIT. Staining was performed after thawed cells, washed them and counted using Trypan Blue, and using a 6-colour panels. The antibodies used were reported in the table below (Table 3)

Table 3. List of monoclonal antibodies targeting Cluster of Differentiation (CD) markers, their clones, fluorochromes, and suppliers used in flow cytometry analysis.

Cluster of Differentiation (CD)	Clone	Fluorochrome	Company
CD3	OKT3	APC	BioLegend (San Diego, CA, USA)
CD4	SK3	FITC	Becton Dickinson (Franklin Lakes, NJ, USA)
CD8	SK1	BV421	BioLegend (San Diego, CA, USA)
PD-1	PE	PD1.3.1.3	Miltenyi Biotec (Bergisch Gladbach, DE)
TIGIT	APC-Cy7	A15153G	BioLegend (San Diego, CA, USA)
CD56	5.1H11	PerCP/Cy5.5	BioLegend(San Diego, CA, USA)

Samples were acquired on BD FAC SLyric flow cytometer (BD-Biosciences San Jose, CA, USA), and compensation was applied using single stained controls and compensation beads (BD™ CompBeads) to calibrate instrument for MFI acquisition. A minimum of 100.000 events per samples were acquired for analysis. Data were analysed using Kaluza Software 2.1 (Beckman Coulter, Brea, CA, USA). Cells were discriminate base on Forward (FCS) versus Side (SSC) scatter, then doublets cells were excluded. A first dot plot was used to distinguish CD3, followed by a second dot plot from the $CD3^+$cells to differentiate $CD4^+$ and $CD8^+$ T cell subsets. Subsequently, the expression of PD-1 and TIGIT was evaluated through three separate dot plots, applied respectively to $CD4^+$, $CD8^+$, and $CD56^+$ cell populations. This allowed for the identification of the following subpopulations: $CD4^+PD\text{-}1^+$, $CD4^+TIGIT^+$, and $CD4^+PD\text{-}1^+TIGIT^+$, $CD8^+PD\text{-}1^+$, $CD8^+TIGIT^+$, and $CD8^+PD\text{-}1^+TIGIT^+$. Fig.12

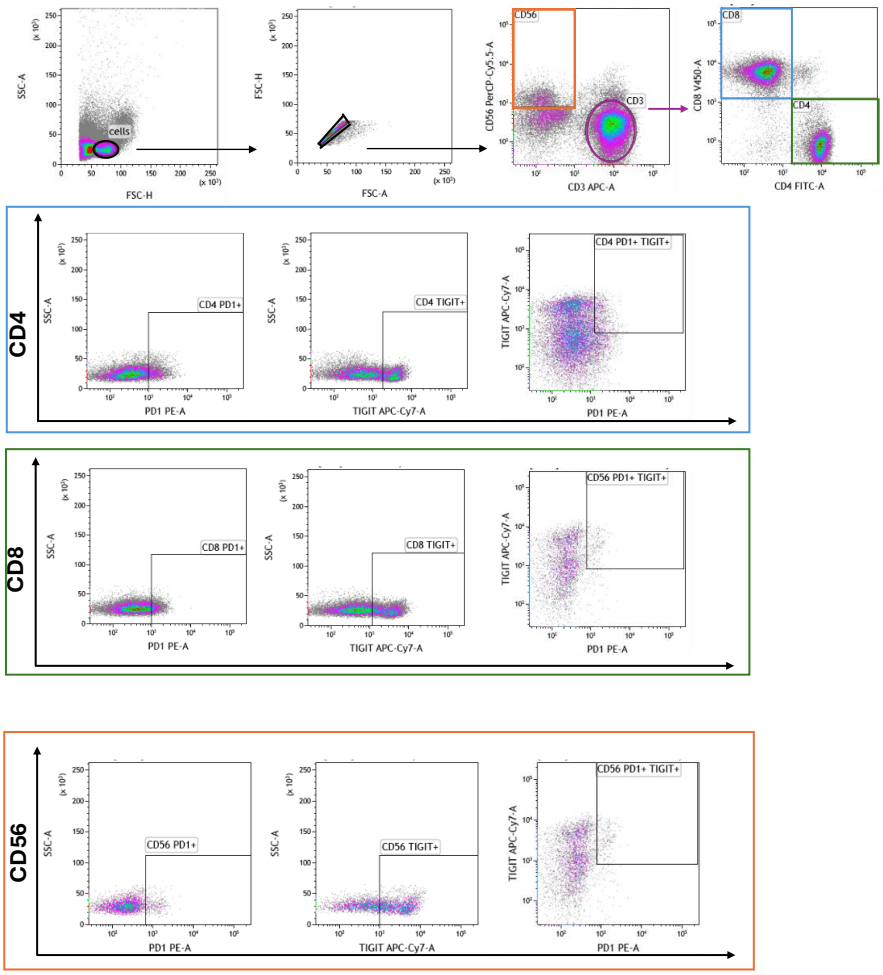

Fig. 12 **Flow cytometry gating strategy for identifying PD-1$^+$ and TIGIT$^+$ expression on CD4$^+$ and CD8$^+$ T cells and CD56$^+$ cells.** Peripheral blood mononuclear cells (PBMCs) were gated based on size and granularity to identify lymphocytes, followed by selection of CD3$^+$ T cells. CD4$^+$ and CD8$^+$ and CD56$^+$ cells subsets were analysed for PD-1 and TIGIT co-expression to assess activation and exhaustion profiles.

In addition, another dot was used to distinguish CD3$^-$ from CD56$^+$ cells, and CD3$^+$CD56$^+$ (NKT LIKE) cells. Then a dot was used based on CD56 expression intensity to distinguish CD56^bright and CD56^dim subsets. Separate dot plots were used to assess PD-1 and TIGIT expression within each of these subpopulations. Fig. 13

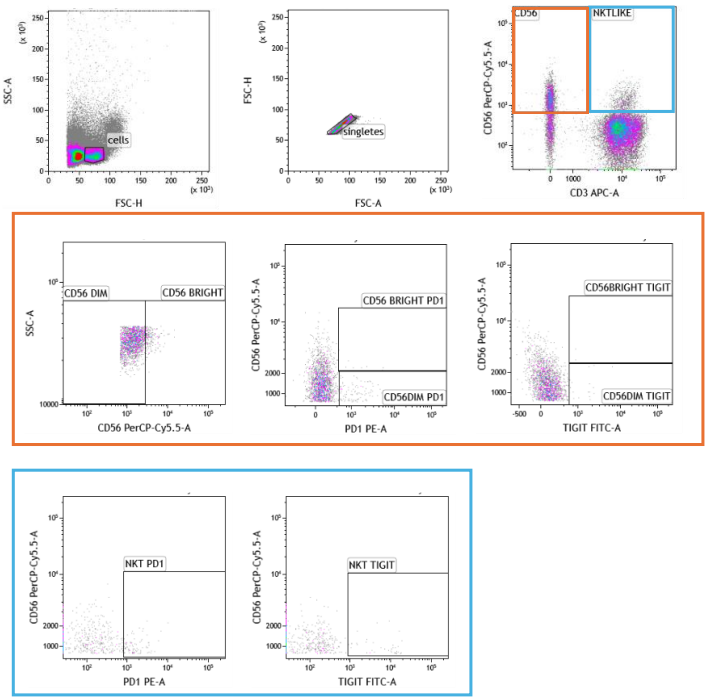

Fig. 13 **Flow cytometry gating strategy for identifying CD56$^+$ subpopulation expressing PD-1 and TIGIT.** Peripheral blood mononuclear cells (PBMCs) were gated based on size and granularity to identify lymphocytes, followed by selection CD56$^+$ cells. CD56$^+$ cells subpopulation were analysed for PD-1 and TIGIT co-expression to assess activation and exhaustion profiles.

4.5 CD8 isolation

CD8$^+$ T cells were isolate from thawed IPF patients and HCs using a manual magnetic labelling protocol with the CD8$^+$ T Cell Isolation Kit (Miltenyi Biotec), according to the manufacturer's instructions. All steps were carried out at 2–8 °C using pre-cooled buffers and equipment to preserve cell viability. Following preparation of a single-cell suspension and counting cells, up to 10^7 total cells were resuspended in 40 µL of magnetic labelling buffer. Subsequently, 10 µL of the Biotin-Antibody Cocktail was added, and the cells were incubated for 5 minutes at 4 °C. Afterward, 30 µL of buffer and 20 µL of the CD8$^+$ T Cell MicroBead Cocktail were added, and the suspension was incubated for an additional 10 minutes at 4 °C. The labelled cells were then resuspended to a minimum volume of 500 µL and applied to an LS Column placed in a magnetic field (MACS

Separator, Miltenyi Biotec). The flow-through containing unlabelled $CD8^+$ T cells were collected. Following isolation, cells were counted using the Trypan Blue exclusion method to assess viability and analysed by flow cytometry to determine expression of CD3 and CD8 surface markers, as well as confirm viability using a live/dead discriminator dye (staining steps are reported by BD Cytofix/Cytoperm™ Fixation/Permeabilization Solution Kit). Table 4.

Table 4. Characteristics of the monoclonal antibodies used for multicolour flow cytometric analysis, including clone, fluorochrome, and manufacturer.

mAB	Clone	Fluorescence	Company
CD3	OKT3	BV510	BioLegend (San Diego, CA, USA)
CD8	REA734	VioBlue	Miltenyi Biotec (Bergisch Gladbach, DE)
Viability		eFluor 506 dye	Invitrogen

Following flow cytometric analysis, 2×10^6 $CD8^+$ T cells were seeded per well in four wells of a 48-well plate, using 500 µL of complete RPMI-1640 modified, with 20nM HEPES and L-gltutamine (Sigma-Aldrich), supplemented with 10% fetal bovine serum (FBS), 1% penicillin-streptomycin, and recombinant human IL-2 at a final concentration of 100 IU/mL to support cell survival and proliferation. Then the cells were allowed to rest at 37°C in 5% atmospheric CO_2 for two hours prior to PD-1 pathway blockade (5µg /mL) (GoInVivo™ Purified anti-mouse CD279 (PD-1) Antibody, BioLegend). Subsequent two hours, $CD8^+$T cells were incubated overnight at 37°C in 5% atmospheric CO_2 with or without anti-PD1. After overnight incubation, isolated $CD8^+$T cells were TCR stimulated using Dynabeads™ Human T-Activator CD3/CD28 (Thermo Fisher scientific) at a bead-to-cell ratio of 1:1, according to the manufacturer's protocol. In parallel, a subset of wells was treated with nintedanib (30 nM) to assess its effect on $CD8^+$ T cell activation and function. All conditions were incubated for 2 days at 37°C in 5% atmospheric CO_2 and stained with flow cytometry antibodies on the end of 2^{th} day. Fig.14

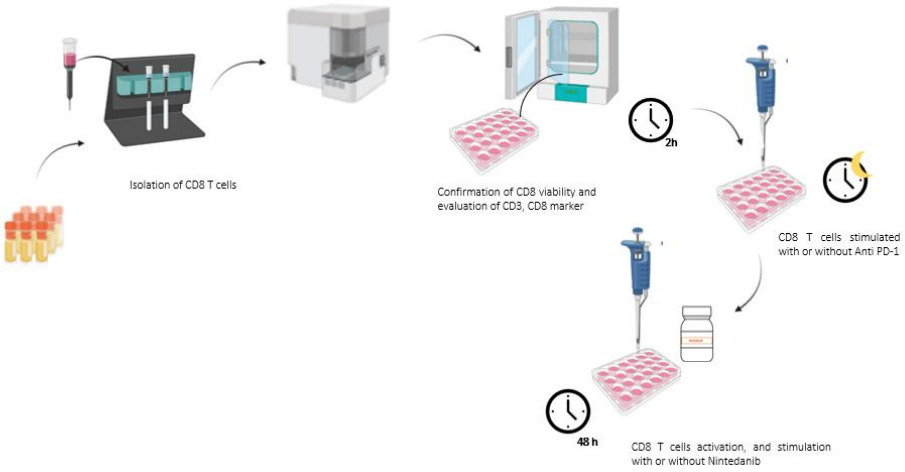

Fig. 14 **Protocol of CD8$^+$ T cells isolation.** CD8+ T cells were isolated from thawed PBMCs, and their purity and viability were confirmed by flow cytometry. Cells were then seeded, and the following day, stimulated and treated with or without anti-PD-1 and nintedanib.

4.6 Flow Cytometry- CD8 cells characterization

Phase 2- Functional ad exhaustion marker expression on CD8 isolated cells

To investigate immune activation, cytotoxicity, and exhaustion profiles of CD8 isolated and stimulate cells, a more complex panel was applied, targeting both surface and intracellular markers including: CD25, CD69, granzyme, perforin, PD-1, CD54, CD107A and viability dye. After cell collection and washing, cells were incubated 30 minutes in the dark at 4°C, following the addition of surface staining flow cytometry antibodies. The cells were than fixed and permeabilized using the intracellular fixation and permeabilization buffer set from BD Cytofix/Cytoperm™ Fixation/Permeabilization Solution Kit for 20 minutes in the dark at 4°C. Succeeding washing, cells were stained with intracellular antibodies for 30 minutes in the dark at 4°C. Data acquisition was performed using Cytek® Northern Lights spectral flow cytometer (Cyteck Biosciences), allowing simultaneous detection of eleven markers using spectral unmixing. Compensation was applied using single stained controls and compensation beads (Cyteck combeads; miltenyi combeads). The antibody panel for this study's phase included

fluorochromes reported in the table below on Fig.15. A minimum of 100.000 events per samples were acquired for analysis. The subsequent data analysis was performed by FCS Express™ 7 (Denovo software), using the same gating strategy applied across all sample Fig. 15

Marker	Clone	Fluorescent Tag	Species	Dilution	Supplier
CD3	OKT3	BV510	Human		BioLegend
CD8	REA734	VioBlue	Human		Miltenyi Biotec
CD25	REA570	APC	Human		Miltenyi Biotec
CD69	FN50	PE	Human		Thermo Fisher Scientific
TIGIT	A15153G	APC-Cy7	Human		BioLegend
CD279 (PD-1)	MIH4	PE-CF594	Human		BD Biosciences
CD107a (LAMP-1)	H4A3	BV605	Human		BioLegend
CD54 (ICAM1)	REA266	Vio Bright B515	Human		Miltenyi Biotec
Granzyme B	GB11	RB545	Human		BD Biosciences
Perforin	dG9	PerCP-Cy5.5	Human		BioLegend
Fixable Viability Dye		eFluor 506	Human		

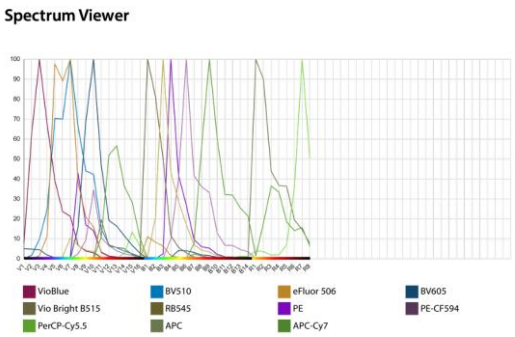

Fig. 15 On the left, characteristics of the monoclonal antibodies used for spectral flow cytometric analysis, including clone, fluorochrome, and manufacturer. On the right, the spectrum viewer of monoclonal antibodies.

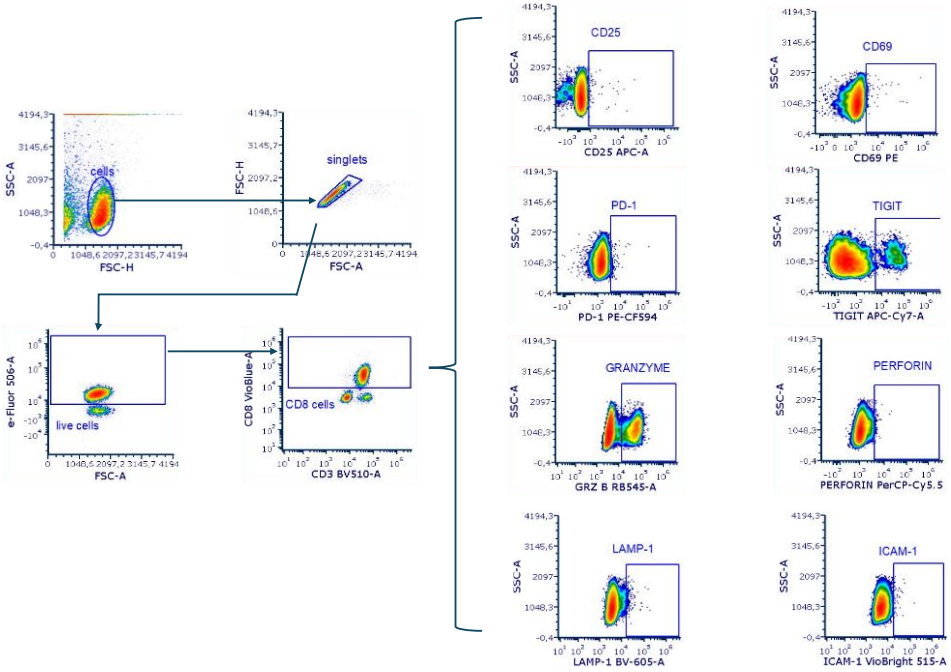

Fig.16 **Flow cytometry gating strategy for identifying CD8⁺ expressing activation markers (CD25 and CD69), immune checkpoints (PD-1 and TIGIT), cytotoxicity markers (granzyme and perforin), degranulation marker (LAMP-1), adhesion marker (ICAM-1)**. Gating strategy for Live cells and singlets were gated out using forward and side scatter properties. Sub-gating for population that are simultaneously expressing CD3 and CD8 were performed to assess CD25, CD69, PD-1, TIGIT, Granzyme, Perforin, LAMP-1 and ICAM-1expression with CD8 cells.

4.7 Cytotoxicity and Proliferation assay

CD8 T cells previous isolated, stimulated and treaded as mentioned above, were plated at $1x10^4$ in sets of triplicates per subject in complete RPMI-1640 modified, with 20nM HEPES and L-gltutamine- supplemented media. CD8⁺ T cells, previously isolated, stimulated, and treated as described above, were assessed for cytotoxic activity using a live-cell imaging assay performed with the live-cell imaging IncuCyte® system (Sartorius). Due to their non-adherent nature, 96-well tissue culture plates were pre-coated with fibronectin (10 µg/mL in PBS) by adding 50 µL per well and incubating at 4°C for 3 hours. The coating solution was then removed, and the plates were air-dried for 30–60 minutes before cell seeding. Prior to plating, CD8⁺ T cells resuspended in complete culture medium- RPMI-1640 modified, were adding of the IncuCyte® Cytotox Green

Reagent, pre-diluted to 2X final working concentration, and the IncuCyte® NucLight Rapid Red Dye (diluted 1:1000). $1x10^4$ cells were plated in set of triplicates per subject to a final volume of 200 µL per well. The plates were immediately placed into the IncuCyte® system, where images were acquired at regular intervals of 2 hours over a 48-hour period. Cells were monitored in real time and quantified using the IncuCyte® Cell-by-Cell Analysis Module, allowing single-cell resolution of fluorescence signal and morphological changes associated with cytotoxicity.

4.8 Lung Function Test

Lung function measurements were obtained following established ATS/ERS guidelines using a Jaeger Body Plethysmograph, with adjustments made for temperature and atmospheric pressure. The assessed parameters included forced expiratory volume in one second (FEV1), forced vital capacity (FVC), and carbon monoxide diffusing capacity (DLCO). Results were reported as percentages of predicted normal values.

4.9 Statistical analysis

Descriptive analysis was performed to evaluate medians and interquartile ranges or means ± standard deviations, as appropriate. A comparison between the two cohort to evaluate difference in markers expression, were performed using a nonparametric one-way analysis of variance (Kruskal–Wallis test). To detect correlations between immunological and clinical findings, the Spearman test was performed. To investigate the global variance in immune marker expression profiles across $CD8^+$ T-cell were performed multivariate analysis including a principal component analysis (PCA) and hierarchical clustering. Moreover, to assess treatment-related modulation of $CD8^+$ T-cell phenotype was performed a non-parametric Friedman test. Post-hoc comparisons were performed using Dunn's multiple comparison test. A $P< 0.05$ was considered statistically significant. Cytotoxicity and proliferation activity of $CD8^+$ T cells was explored using a two-way ANOVA followed by Tukey's multiple comparisons test. All experiments were repeated at least three times. Figures were constructed using GraphPad Prism version 10 (GraphPad Software) and Jamovi software 2.3.

CHAPTER 5: Results

5.1 Clinical feature of study population

The main characteristics of our study population are reported in Table 5. A total of 52 patients and 12 HCs were enrolled in the study. Of these, 47 patients and 8 HCs were retrospectively evaluated for T cells immunophenotyping. In the second part of the study, 5 additional patients affected by IPF and 4 HCs were enrolled to perform the analysis ofCD8 T cells and testing treatment effects.

Table 5. Summary of demographic characteristics and pulmonary function test results in idiopathic pulmonary fibrosis (IPF) patients and healthy controls (HCs).

	IPF (n = 52)	*HCs (n = 12)*
Sex (F/M)	15/37	6/6
Age (median)	74[68-79]	61 [52 -70]
Smoking (smoker/never/former)	5/15/32	2/8/2
Lung function parameters (median ± standard deviation)		
FEV1%	83.3±21.10	
FVC%	76.6±20.13	
DLCO%	55.6±31.05	

5.2 Increase percentages of cytotoxic CD8 and NK cells emerged in IPF patients.

To delineate the role of co-inhibitory molecules in IPF, we first examinate PD-1 and TIGIT expression on systemic $CD4^+$, $CD8^+$ and $CD56^+$ T cells. Notably, a significant increase in the frequency of $CD8^+$ and $CD56^+$ T cells was observed in patients with IPF compared to healthy controls (HCs) ($p < 0.001$). In order to establish the exhaustion of these cells ,we assessed the surface expression of PD-1 and TIGIT, which were markedly upregulated on both $CD8^+$ (*$CD8^+PD\text{-}1^+$ and $CD8^+TIGIT^+$*, $p < 0.001$, respectively; PD-1 MFI: 1,154.155417, TIGIT MFI: 3,111.384375) and $CD4^+$ T cells (*$CD4^+PD\text{-}1^+$*, $p = 0.034$ MFI: 1,508.846042; *$CD4^+TIGIT^+$*, $p = 0.002$ TIGIT MFI:2,254.543125). In contrast,

$CD56^+$ T cells showed a significant increase in TIGIT expression compared to HCs ($p = 0.022$, MFI: 4,441.51), with no change in PD-1 expression. indicating increased per-cell expression. Moreover, all three T cell subsets showed a significantly higher co-expression of PD-1 and TIGIT in IPF patients than HCs: $CD4^+PD\text{-}1^+TIGIT^+$, $CD8^+PD\text{-}1^+TIGIT^+$, and $CD56^+PD\text{-}1^+TIGIT^+$ ($p < 0.001$, $p < 0.001$, p=0.039, respectively) supporting the presence of a systemically exhausted or chronically activated T cell phenotype in IPF. Consistently, MFI values of PD-1 and TIGIT were highest in the double-positive ($PD\text{-}1^+TIGIT^+$) populations within each subset ($CD4^+$, $CD8^+$, $CD56^+$: 2,041.44; 2,211.78; 7,500.99), further indicating heightened co-inhibitory signalling. Fig.17

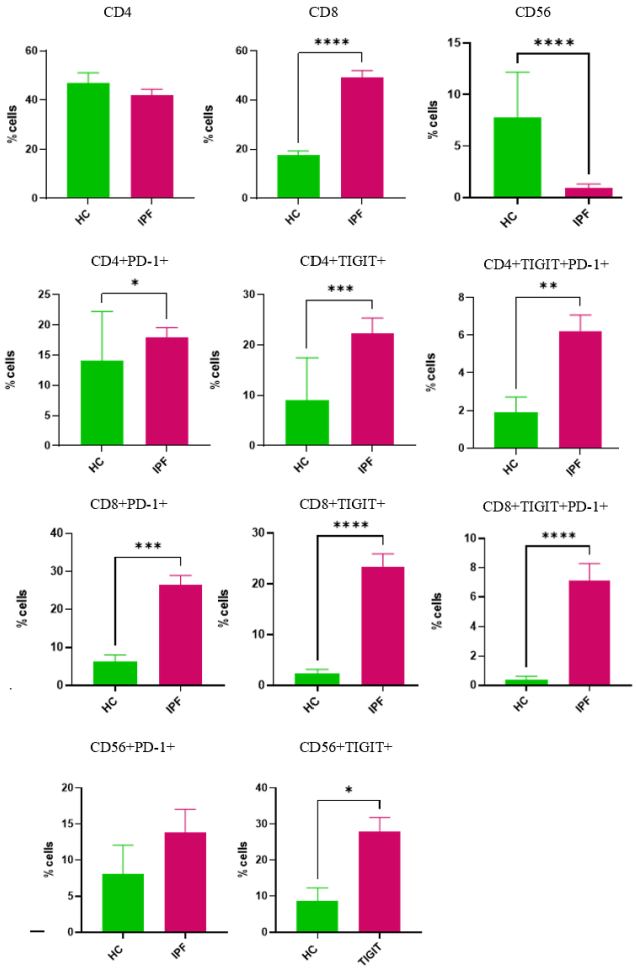

Fig.17 **Increased PD-1 and TIGIT surface expression in IPF $CD4^+$, $CD8^+$ and $CD56^+$ T cells.** PD-1 and TIGIT expression in cells from IPF patients compared to Healthy Controls (HCs, n= 8; IPF, n= 47). $^*p<0.005$, $^{**}p<0.01$, $^{***}p<0.001$, $^{****}p<0.0001$.

5.3 The expression of TIGIT on NK cell subsets resulted high in patients with IPF

Analysis of $CD56^{+}$ NK cell subpopulations revealed significant alterations in checkpoint receptor expression in patients with IPF compared to HCs. Specifically, TIGIT expression was significantly increased in both CD56 ^{bright} ($p = 0.036$) and CD56 ^{dim} ($p < 0.001$) subsets in IPF. These two subsets are known to differ functionally, with $CD56^{bright}$ NK cells primarily involved in immunoregulatory cytokine production, while CD56 ^{dim} NK cells exhibiting potent cytotoxic activity. The increase expression of TIGIT suggest enhanced inhibitory signalling across both subsets. Furthermore, invariant natural killer T (iNKT) cells, defined by co-expression of CD3 and CD56, demonstrated significantly higher expression of PD-1 ($p = 0.006$) and TIGIT ($p < 0.001$) in IPF patients compared to HCs. The expression of NKT-like cells was also increased in IPF ($p = 0.019$). These findings indicate a broad upregulation of inhibitory checkpoint receptors in NK and NKT cell populations in IPF, potentially contributing to immune dysregulation associated with disease pathogenesis. Fig. 18

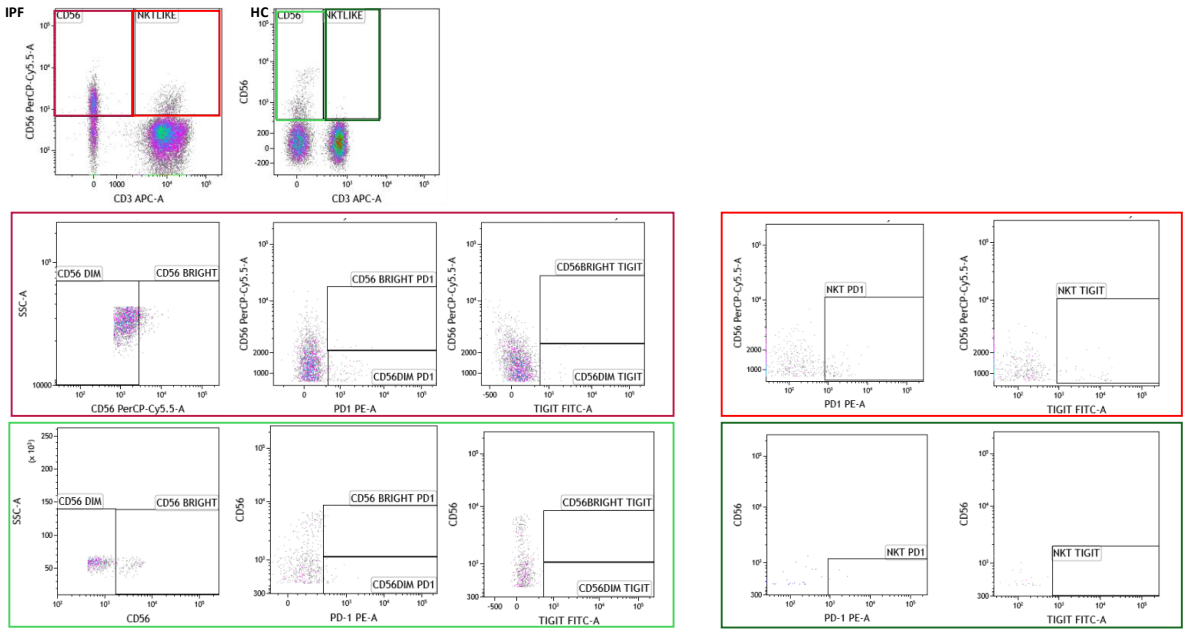

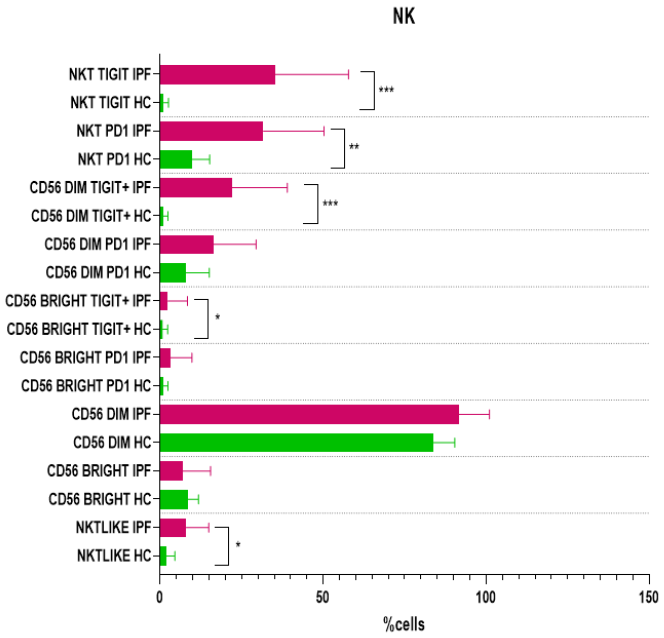

Fig.18 **Enhanced TIGIT and PD-1 Expression in CD56^bright, CD56^dim, and NKT Cells in Idiopathic Pulmonary Fibrosis.** TIGIT and PD-1 expression in cells from IPF patients compared to Healthy Controls (HCs, n= 8; IPF, n= 47). $^{*}p<0.005$, $^{**}p<0.01$, $^{***}p<0.001$, $^{****}p<0.0001$.

5.4 Immune Cell Crosstalk and Checkpoint Regulation

The immune imbalance observed in IPF patients was supported by a strong inverse correlation between $CD4^+$ and $CD8^+$ T cells ($p<0.0001$; $r = -0.865$), suggesting reciprocal changes in these subsets. $CD4^+$ T cells expressing PD-1 positively correlated with $CD8^+PD\text{-}1^+$ cells ($p = 0.001$; $r = 0.461$), while $CD4^+TIGIT^+$ cells showed a strong positive correlation with $CD8^+TIGIT^+$ cells ($p<0.0001$; $r = 0.760$). Similarly, $CD4^+$ T cells co-expressing PD-1 and TIGIT positively correlated with $CD8^+PD\text{-}1^+TIGIT^+$ cells ($p<0.0001$; $r= 0.717$), indicating coordinated inhibitory receptor expression across T cell subsets. Among $CD56^+$ cells, there was an inverse correlation between total $CD56^+$ cells and $CD56^+$ cells expressing PD-1 ($p=0.031$; $r=-0.326$). Fig.19

Despite the limited sample size in HCs (n=8), several significant correlations were observed, suggesting tightly regulated immune checkpoint expression under homeostatic conditions. $CD4^+PD\text{-}1^+$ T positively correlated with $CD4^+TIGIT^+$ ($p = 0.058$; $r =$

0.714).CD8^{+}PD-1^{+} cells also showed strong correlations with CD8^{+}TIGIT^{+} cells (p = 0.007; r = 0.881).A strong correlation was also seen between CD4^{+}TIGIT^{+} and CD8^{+}TIGIT^{+} cells (p = 0.011; r = 0.857), reflecting a coordinated inhibitory profile. CD4^{+} T cells co-expressing PD-1 and TIGIT correlated with CD8^{+}PD-1^{+}TIGIT^{+} cells (p < 0.0001; r = 0.776) Fig.19.

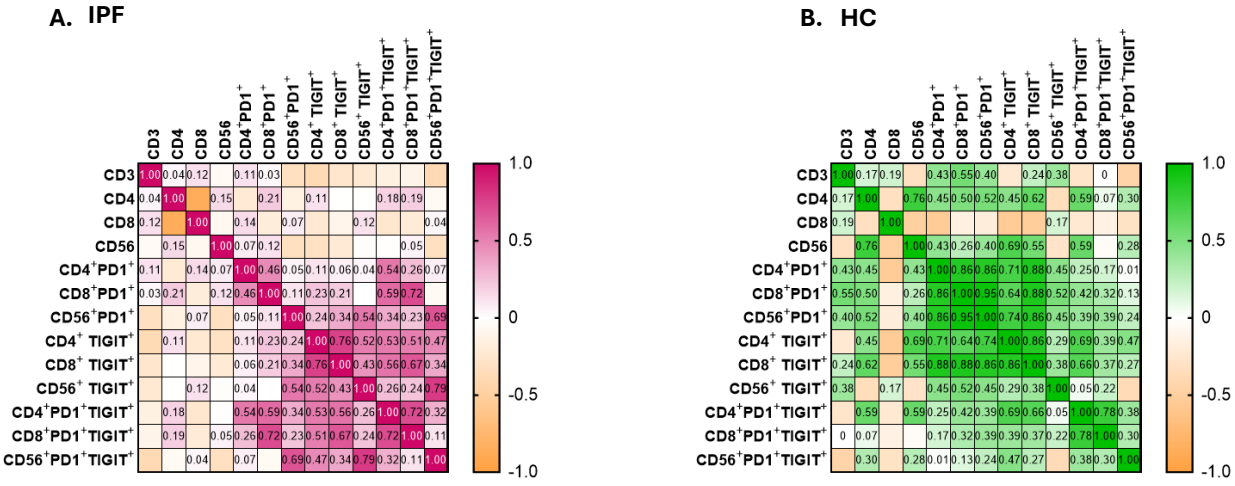

Fig.19 **Correlation matrix of immune checkpoint expression in T cell subsets of IPF patients.** Spearman correlation matrix illustrating the pairwise correlations between frequencies of CD4^{+}, CD8^{+}, and CD56^{+} T cells, including subsets expressing the immune checkpoints PD-1 and TIGIT, in patients with IPF (Fig. A) and HCs (Fig. B). The colour scale in the legend indicates the strength and direction of correlation (Spearman's rho).

5.5 Principal Component Analysis reveals distinct treatment- and disease-associated segregation of CD8^{+} T-cell phenotypes in IPF.

To assess the overall distribution of immune marker expressed by CD8 T and explore potential clustering patterns principal component analysis (PCA) and hierarchical clustering were performed under four experimental conditions: unstimulated (UNSTIM), nintedanib (NINT), anti-PD-1, and combined anti-PD-1 plus nintedanib (anti-PD-1 + NINT).The initial PCA was designed to highlighted treatment-specific variance without the influence of the unstimulated condition. The integrated PCA comparing all

experimental condition (anti-PD1, nintedanib, and combination) in the two group of the study (HCs and IPF patients), (Fig.20) shows the separation of individual across the first two principal components, which together account for 57.4% of the total variance (PC1: 34.9%, PC2: 22.5%). The samples tend to cluster according to their treatment and disease status, with partially overlapping yet distinguishable groupings among CD8 T cells from IPF patients and HCs treated with anti-PD-1, nintedanib, and anti-PD-1 plus Nintedanib. The biplot (Fig.20) further highlights the contribution of key variable, including CD69, PD-1, TIGIT, ICAM-1, Granzyme B, Perforin and LAMP-1, which drive the differentiation along the main principal components.

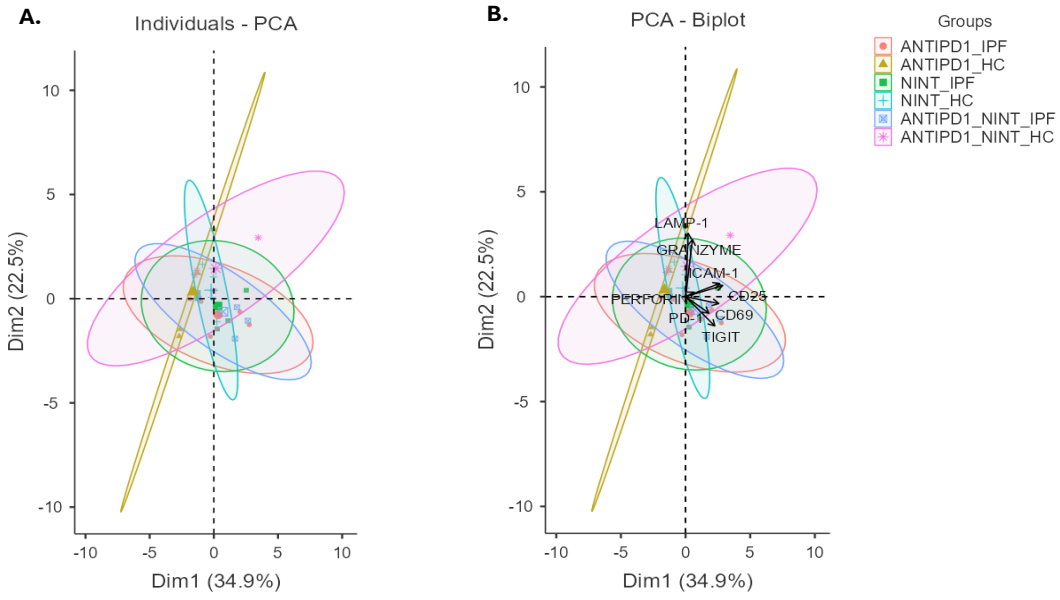

Fig.20 **Principal component analysis (PCA) of CD8 T cells across treatments and disease status. A:** Individual samples from unstimulated (UNSTIM), nintedanib (NINT), anti-PD-1, and combined anti-PD-1 + NINT conditions in healthy controls (HCs) and IPF patients, projected onto the first two principal components (PC1: 34.9%, PC2: 22.5%), explaining 57.4% of total variance. Samples cluster primarily by treatment and disease status. **B:** Biplot showing key variables driving separation, including CD69, PD-1, TIGIT, ICAM-1, Granzyme B, Perforin, and LAMP-1.

In a subsequent analysis, the PCA was extended to include all experimental groups—stimulated and unstimulated—to evaluate how the inclusion of baseline samples affects clustering.

In the unstimulated condition Fig. 21. A., PCA revealed a separation between IPF and HC samples along the first principal component (PC1, explaining 53.4% of the variance), indicating differences in basal activation and cytotoxic marker expression. Variables contributing mainly to this segregation included TIGIT, CD69, CD25 and Perforin, which were more closely associated with the IPF group, suggesting a basal activation or early exhaustion state of $CD8^+$ T cells even in the absence of stimulation.

Following anti-PD1 stimulation Fig.21. B., PC1 (48.3%) and PC2(25.4%) showed the main sources of variance. A separation between IPF and HC samples was observed primarily along PC1, reflecting divergent transcriptional and phenotypic response to PD-1 inhibition. The markers most strongly associated with this component included TIGIT, CD69, CD25, and Perforin.

In contrast, exposure to nintedanib Fig.21. C., PC1 (42.2%) and PC2 (26.7%), maintained a distinct segregation between IPF and HCs with PD-1, TIGIT, CD69, and CD25 associated with IPF, while Granzyme, Perforin, and LAMP-1 were more aligned with HCs. This suggests that nintedanib treatment sustains a partially activated, regulatory phenotype in IPF, whereas HCs retain a more cytotoxic signature.

In the combined treatment condition (anti-PD-1 plus Nintedanib) Fig.21. D., PC1(33.4%) and PC2 (27.7%), the clustering pattern distinguished IPF samples from HCs. PCA demonstrated the most pronounced discrimination between IPF and HC samples along PC1 (33.4%). The IPF cluster was associated with PD-1, TIGIT, and Perforin, while HCs showed positive loadings for CD25, CD69, ICAM-1, LAMP-1, and Granzyme**.** These data indicate that dual modulation does not normalize the IPF $CD8^+$ phenotype but instead amplifies its divergence from HCs.

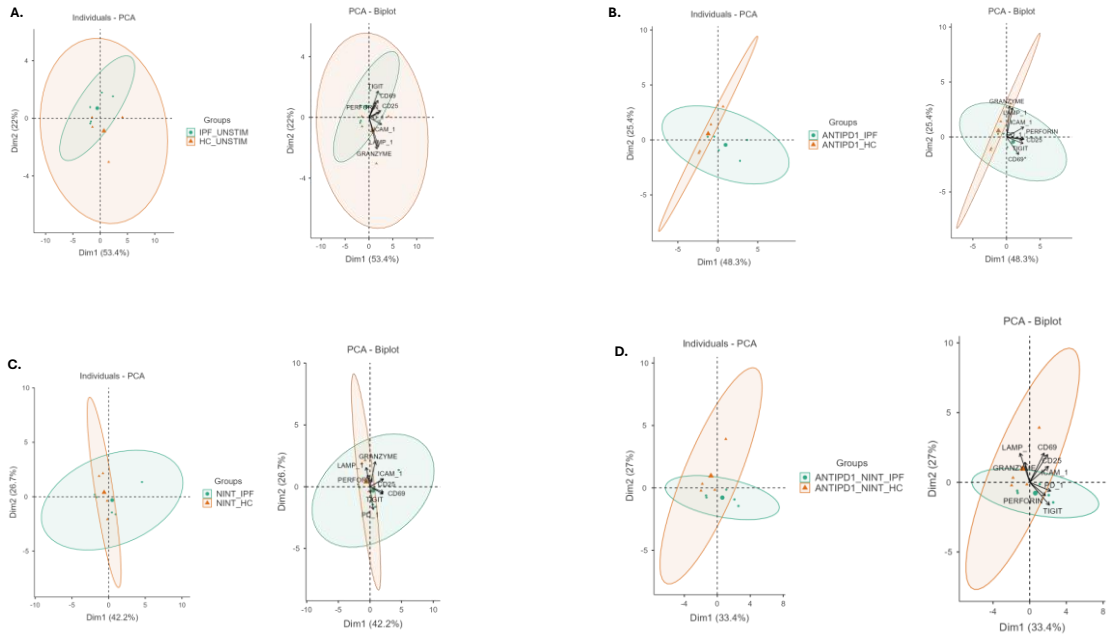

Fig.21 **Principal component analysis (PCA) of CD8⁺ T cells isolated from idiopathic pulmonary fibrosis (IPF) patients (n = 5) and healthy controls (HCs, n = 4) under four experimental conditions**: unstimulated (UNSTIM), nintedanib (NINT), anti-PD-1, and combined anti-PD-1 + nintedanib (anti-PD-1 + NINT). Each point represents an individual donor, and 95% confidence ellipses denote the distribution of each group. Biplots display the direction and magnitude of the variables contributing most strongly to sample separation. Percentages on the axes indicate the proportion of variance explained by each principal component.

5.6 Unsupervised clustering analysis of treatment-induced changes in CD8⁺ T-cell phenotype

Hierarchical clustering was performed using the percentages of cells express Granzyme B, Perforin, LAMP-1, PD-1, TIGIT, CD69, CD25, and ICAM-1. Both clustering of samples was conducted using Euclidean distance and complete linkage methods.

The hierarchical clustering of markers Fig.22. A., based on similarity in expression patterns across all samples and condition, revealed four principal groups. Interestingly, the first and second groups, a cytotoxicity-associated clusters including LAMP-1, Granzyme B, and perforin. Their tight grouping indicates coordinated regulation of cytolytic effector functions across the experimental conditions.

The third that was an activation cluster including CD25, CD69 and ICAM-1, representing markers of activation and adhesion, suggesting that these molecules share similar expression dynamics in response to treatments.

The latter, an inhibitory receptor cluster comprising PD-1 and TIGIT, two inhibitory checkpoint receptors that displayed distinct expression patterns relative to the cytotoxic and activation clusters, highlighting their independent regulatory behaviour.

The heatmap analysis Fig.22. B., further illustrate alterations in immune-related marker expression across IPF and HCs $CD8^+$ T cells in different conditions. Elevated expression of the inhibitory receptors TIGIT and PD-1 was observed, suggesting the presence of T-cell exhaustion or regulatory suppression in the fibrotic microenvironment. Moreover, increased expression of activation markers CD69 and CD25 indicated persistent immune activation, consistent with ongoing antigenic stimulation. While the expression of cytotoxic and degranulation-associated genes, including granzyme, perforin, and LAMP-1, appeared variable and generally reduced compared to activation markers in the IPF, suggesting that although T cells are activated, their effector function may be impaired.

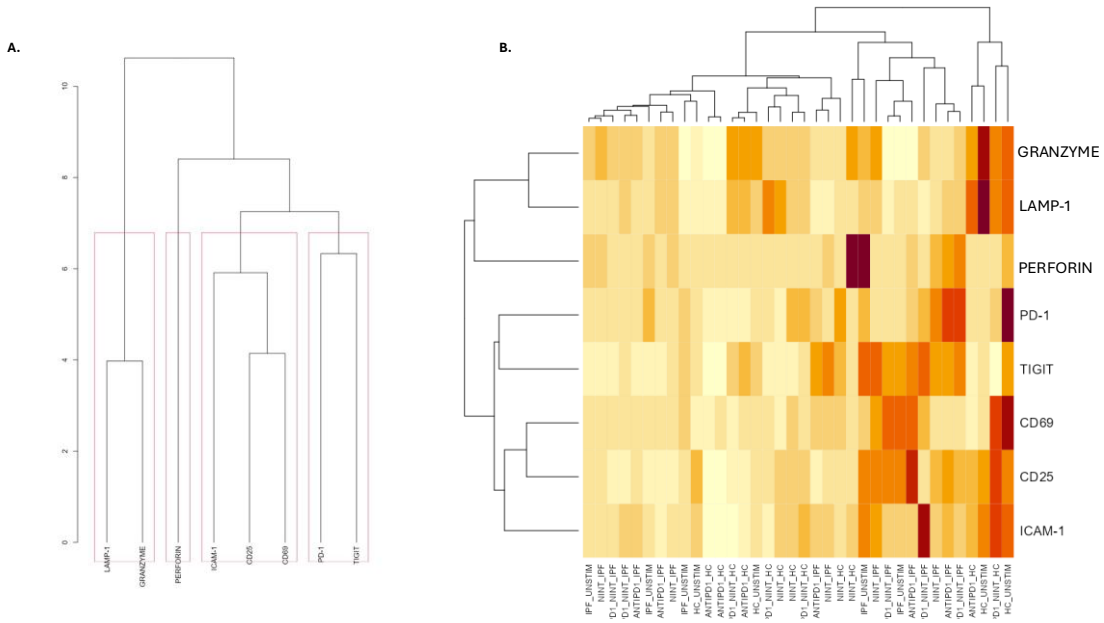

Fig.22 **Hierarchical clustering and heatmap analysis of $CD8^+$ T-cell markers in IPF patients (n = 5) and HCs, n = 4 across four experimental conditions (unstimulated, nintedanib, anti-PD-1, and anti-PD-1 + nintedanib). A:** Dendrogram of marker clustering based on Euclidean distance, highlighting four main clusters corresponding to cytotoxic/degranulation (LAMP-1,

Granzyme B, Perforin), activation/adhesion (ICAM-1, CD25, CD69), and inhibitory checkpoint (PD-1, TIGIT) signatures. **B:** Heatmap of normalized marker expression across samples. Each column represents an individual donor in each condition; colour intensity reflects relative expression levels (yellow = low, dark red = high). IPF and HC groups exhibit distinct clustering patterns, consistent with differential activation states.

5.7 Functional validation of treatment effects on $CD8^+$ T-cell phenotype in IPF

To assess treatment-related modulation of $CD8^+$ T-cell phenotype, a non-parametric Friedman test was performed on samples from patients with IPF; n = 5 and HCs; n = 4, under four experimental conditions: unstimulated (unstim), anti-PD1, nintedanib (Nint), and combined anti-PD1 + nintedanib. Analyses were conducted separately for each group and for each functional markers (activation, exhaustion, cytotoxicity, adhesion). Post-hoc comparisons were performed using Dunn's multiple comparison test.

Activation markers

In IPF-derived $CD8^+$ T-cell, CD25 not showed significantly across conditions in either IPF or HC samples, despite Fig.23 illustrate an increasing trend of expression in IPF patients. While CD69 expression showed significant modulation across treatment conditions (Fig.22.B). Post-hoc testing revealed a significant difference between anti-PD1 and nintedanib ($p = 0.02$), with higher frequencies of $CD69^+$ $CD8^+$ T cells observed following nintedanib exposure. In healthy controls, CD69 expression did not reach statistical significance, although a mild, non-significant increase was observed following nintedanib treatment.

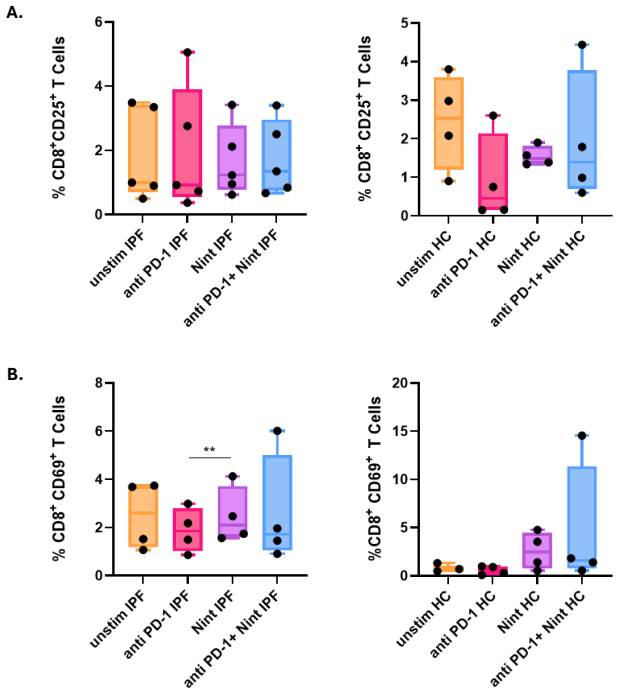

Fig.23 **Activation markers (CD25 and CD69) in CD8⁺ T-cell from IPF patients and healthy controls under different treatment conditions.** Box-and-whisker plots (showing median, interquartile range, and individual data points) depict the frequency of CD25⁺ (on the top, A.) and CD69⁺ (on the bottom, B.) CD8⁺ T cells isolated from IPF patients (n = 5) and healthy controls (HCs; n = 4) under four conditions: unstimulated (Unstim), anti-PD1, Nintedanib (Nint), and combined anti-PD1 + Nintedanib. Statistical significance was assessed using the Friedman test with Dunn's multiple comparison test ($p < 0.05$).

Exhaustion markers

In IPF samples, PD-1 and TIGIT frequencies remained stable across all treatment conditions. A non-significant decrease was observed in PD-1⁺ CD8⁺ T cells following combination treatment (anti-PD1 + nintedanib), suggesting a possible trend toward reduced inhibitory signalling. Across all treated conditions, PD-1⁺ CD8⁺ T-cell frequencies tended to decrease relative to unstimulated cells, although these changes did not reach statistical significance. In HCs, PD-1 expression showed a near-significant trend ($p = 0.05$) across treatments, with a tendency toward increased PD-1⁺ CD8⁺ T cells following anti-PD1 stimulation compared with the unstimulated condition (Fig.23.A.). TIGIT expression remained unchanged in both IPF and HCs groups (Fig.23.B.).

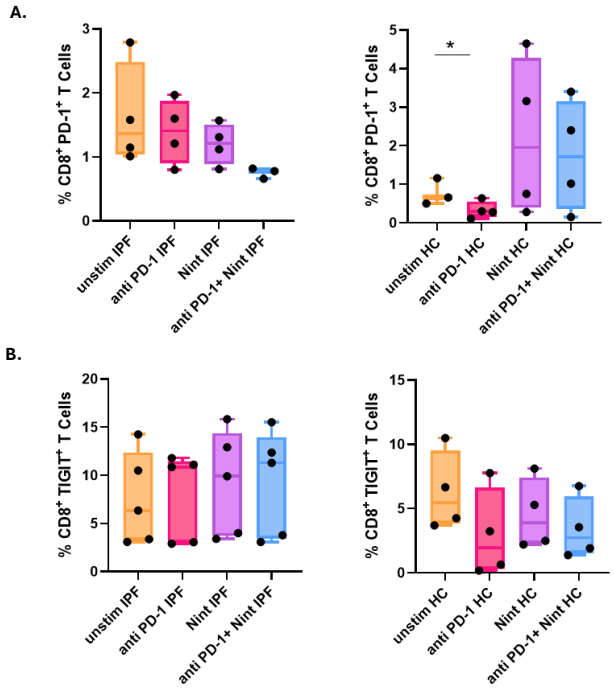

Fig.24 **Exhaustion markers (PD-1 and TIGIT) in CD8⁺ T cells from IPF and healthy controls.** Box-and-whisker plots with overlaid data points represent PD-1⁺ (top, A.) and TIGIT⁺ (bottom, B.) CD8⁺ T-cell frequencies across treatment conditions. Statistical significance was assessed using the Friedman test with Dunn's multiple comparison test ($p < 0.05$).

Cytotoxicity and adhesion markers

In IPF CD8⁺ T cells, the Friedman test revealed significant modulation of Granzyme B expression. Post-hoc analyses identified significant pairwise differences between unstimulated vs. nintedanib (p = 0.05) and anti-PD1 vs. nintedanib (p = 0.05), indicating that nintedanib induces a marked increase in Granzyme B⁺ CD8⁺ T cells relative to both baseline and anti-PD1 conditions. In HCs, Perforin was significantly decreased following anti-PD1 stimulation compared with unstimulated cells (p = 0.02). Fig.25

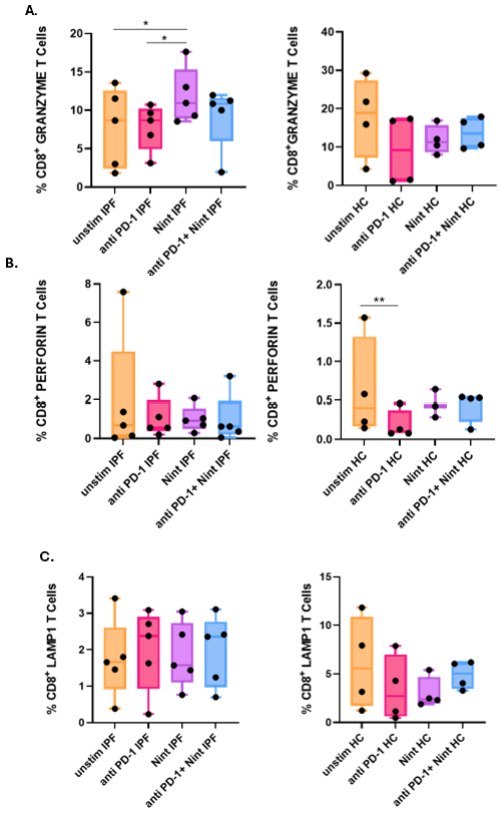

Fig.25 **Cytotoxicity markers (Granzyme B, Perforin, and LAMP-1) in CD8$^+$ T cells from IPF and healthy controls.** Box-and-whisker plots show the distribution of Granzyme B$^+$ (A.), Perforin$^+$(B.), and LAMP-1$^+$ (C.) CD8$^+$ T cells across the four treatment conditions. Statistical significance was assessed using the Friedman test with Dunn's multiple comparison test ($p < 0.05$).

A non-significant trend toward increased ICAM-1$^+$ CD8$^+$ T cells was observed in the combination treatment (anti-PD1 + nintedanib) relative to single-agent conditions, particularly in the IPF group. Fig.26

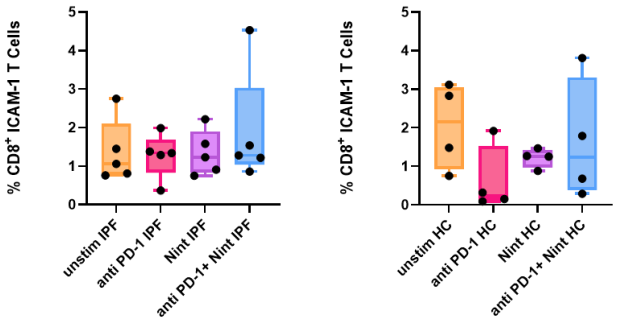

Fig.26 **Adhesion marker (ICAM-1) in CD8⁺ T cells from IPF and HCs**. Box-and-whisker plots with individual data points represent ICAM-1⁺CD8⁺ T-cell frequencies under the four experimental conditions. Statistical significance was assessed using the Friedman test with Dunn's multiple comparison test ($p < 0.05$).

5.8 Modulation of CD8+ T Cell Cytotoxic Activity by anti-PD-1 and Nintedanib in IPF and HCs.

In the IPF group, a significant increase in cytotoxicity was observed in unstimulated CD8+ T cells compared to those stimulated with anti-PD-1 (mean difference = 1361; 95% CI: 360.4 to 2362; $p < 0.01$). Additionally, CD8⁺ T cells stimulated with either anti-PD-1 or nintedanib showed reduced cytotoxic activity compared to the administration of combination of anti-PD-1 and nintedanib (mean difference = -2054, 95% CI: -3052 to -1056, $p < 0.0001$; and mean difference = -1598, 95% CI: -2522 to -674.1, $p < 0.0001$, respectively). (Fig.27.A)

In contrast, the HC group showed a strong response to treatments: significant increase in cytotoxicity observed in all treated CD8⁺ T cells compared to unstimulated cells were observed. : anti-PD-1 (mean difference = 1721; 95% CI: 401.5 to 3041; $p = 0.0047$), nintedanib (mean difference = 1826; 95% CI: 506.6 to 3146; $p = 0.0023$), and the combination treatment (mean difference = 4031; 95% CI: 2711 to 5351; $p < 0.0001$). However, CD8⁺ T cells treated with either anti-PD-1 or nintedanib had significantly lower cytotoxicity than the combination treatment (mean difference = 2310, 95% CI: 989.9 to 3630, $p < 0.0001$; and mean difference = 2205, 95% CI: 884.8 to 3524, $p = 0.0001$, respectively). (Fig.27. C.)

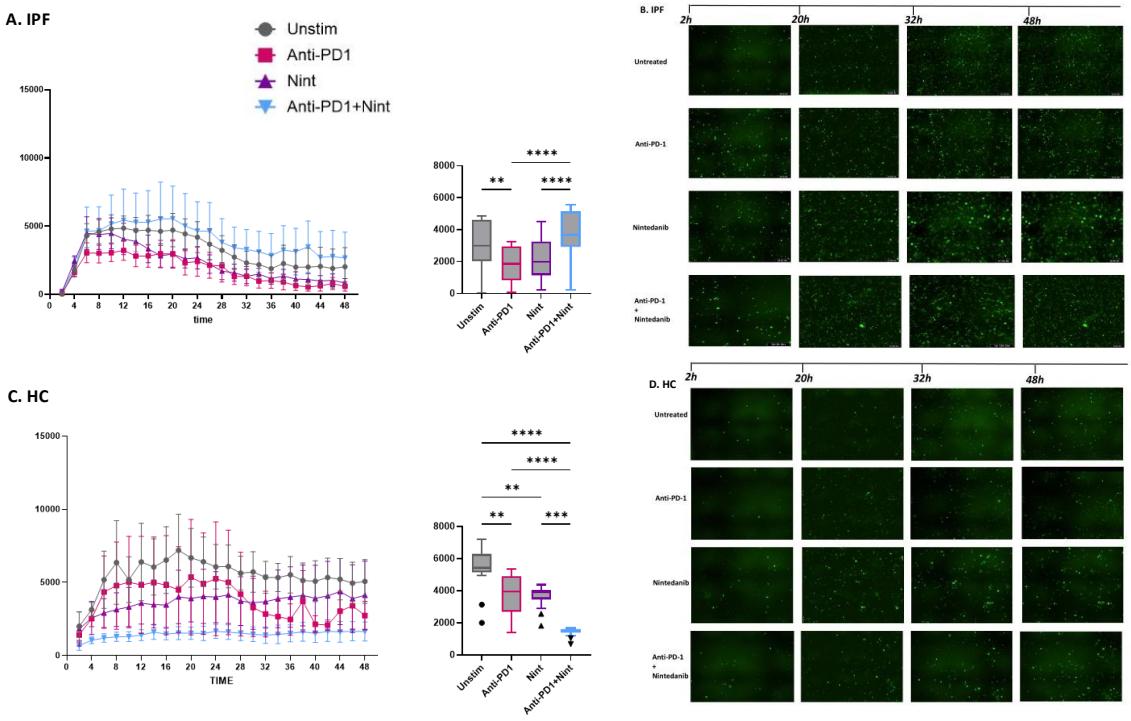

Fig.27 **Anti-PD-1, nintedanib, and their combination modulate the cytotoxic activity of CD8+ T cells in IPF and healthy controls (HCs).** Cytotoxicity of $CD8^+$ T cells from (A-B) IPF patients and (C-D) HCs was measured following 48 hours of treatment with anti-PD-1, nintedanib, or their combination. On the left, points & connecting lines represent individual cell responses over time. On the right, histograms depict the mean cytotoxicity levels for each treatment group.

5.9 Modulation of CD8+ T Cell Proliferation Following anti-PD-1 and Nintedanib treatment in IPF and Healthy Controls.

In the IPF group, proliferation significantly increased in CD8+ T cells treated with nintedanib compared to unstimulated cells (mean difference = -385,2; 95% CI: -627.1 to -143.4; p = 0.0003). Furthermore, nintedanib treatment induced a significant increase in proliferation compared to anti-PD-1 (mean difference = -283.4; 95% CI: -525.3 to -41.52;

p = 0.0144). Moreover, $CD8^+$ treated with nintedanib showed an increase rate of proliferation compared to cells treated the combination treatment (anti-PD-1 + nintedanib) (mean difference = 339,3; 95% CI: 96.00 to 582.6; p = 0.0022).

Similarly, in the HCs group, unstimulated $CD8^+$ resulted in a significant increase of proliferation compared to nintedanib treatment (mean difference = 14,675; 95% CI: 274.4 to 29,076; *p = 0.0439*), and the combination treatment (anti-PD-1 + nintedanib) (mean difference = 19,041; 95% CI: 4640 to 33,442; p = 0.0040).

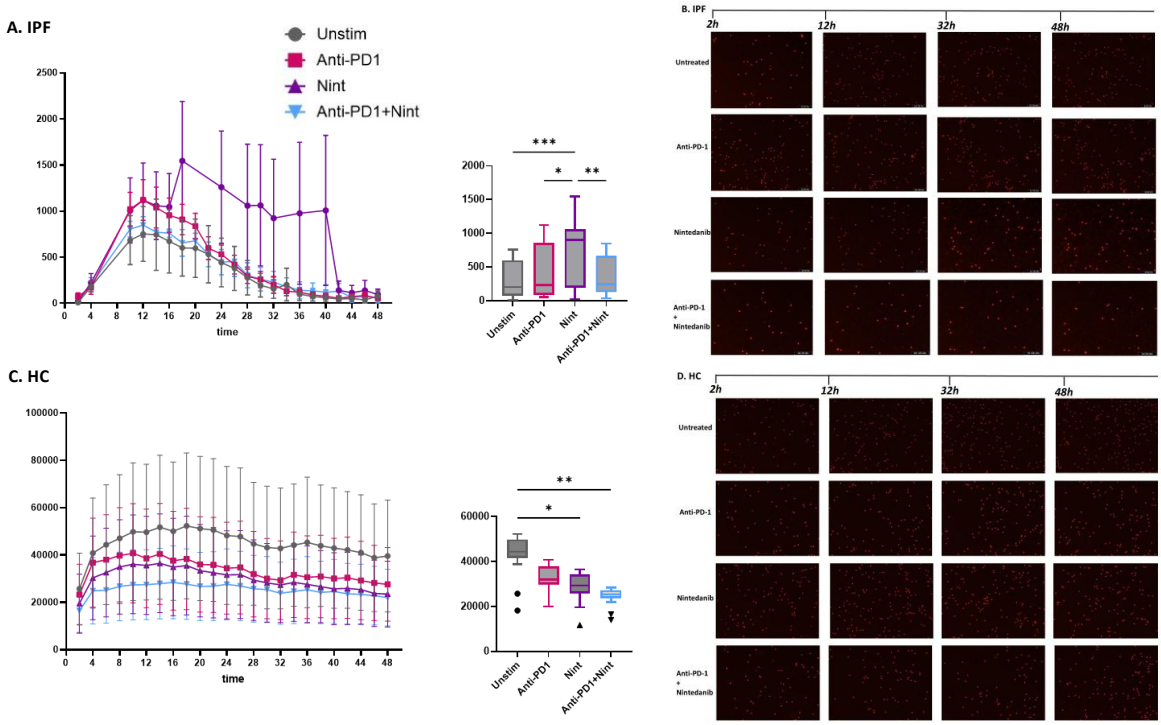

Fig.28 **Anti-PD-1, nintedanib, and their combination modulate the Proliferation of $CD8^+$ T cells in IPF and healthy controls (HCs).** Proliferation of CD8+ T cells from (A-B) IPF patients and (C-D) healthy controls (HCs) after 48 hours of treatment with anti-PD-1, nintedanib, or their combination.

CHAPTER 6: Discussion

IPF is a chronic, progressive interstitial lung disease that leads to irreversible fibrosis and progressive loss of pulmonary function. The pathogenesis of IPF is characterized by persistent epithelial injury, abnormal repair processes, and excessive fibrotic remodelling of the lung interstitium, driven by a dysregulated immune response (100) (101). Although traditionally viewed as a non-inflammatory disease, growing evidence indicate that immune cells, of both innate and adaptive immunity, play a central role in disease progression (102) (64).

In this context, our study aimed to provide new insights into systemic immune dysregulation related to CD8+ cells associated with their alteration following anti-PD-1 and nintedanib administration, as both agents have been implicated in modulating immune homeostasis and fibrotic remodelling processes central to the pathogenesis of IPF

From our first analysis on a large cohort of IPF patients, our data showed a systematic upregulation of co-inhibitory receptors PD-1 and TIGIT across $CD4^+$, $CD8^+$, and $CD56^+$ lymphocytes subsets (both $CD56^{bright}$ and $CD56^{Dim}$) in IPF, confirming a widespread immune exhaustion or chronic activation. These data align with previous reports showing increasing PD-1 T-cell frequencies in both bronchoalveolar lavage and PBMC samples from IPF patients (103) (104) (71).

In accordance with our data, Cruz et al.et al demonstrated that, both CD56 cell subsets – the more immature $CD56^{bright}$, and cytotoxic $CD56^{dim}$ exhibited enhanced expression of inhibitory receptors, suggesting that chronic immune activation may compromise both regulatory and effector NK functions (70).

TIGIT expression of cytotoxic cell compartment of immune system (both CD8 and CD56) of IPF patients was partially described before. The overexpression of TIGIT, particularly increased in $CD8^+$ T cells and CD56 cells, supports the hypothesis that additional inhibitory axes modulate cytotoxic immune responses in IPF (105).

In studies on non–small cell lung cancer, was demonstrated that TIGIT is induced earlier than PD-1 during $CD8^+$ T-cell activation, identifying it as an initiating checkpoint in the exhaustion process (105). In line with these studies, our findings suggest that persistent

TIGIT upregulation in IPF reflects an inefficacy inhibitory response to chronic immune stimulation, contributing to progressive lymphocyte dysfunction within the fibrotic lung microenvironment.

The co-expression of PD-1 and TIGIT observed in our study highlights the presence of coordinated inhibitory signalling networks. Our results may reflect a comparable exhaustion-like state induced by persistent pulmonary injury and antigenic stimulation, that may induce an exhaustion-like state within T-cells limiting effective immune surveillance and fostering a microenvironment conducive to fibrosis progression. Similar dual checkpoint expression has been widely reported in tumour-infiltrating lymphocytes, where PD-1^{+}TIGIT^{+} CD8- T cells display a transcriptional and metabolic profile consistent with functional exhaustion—characterized by reduced effector cytokine production and upregulation of exhaustion-associated transcription factors (106) (107).

We noted a strong correlation between PD-1 and TIGIT expression across CD4^{+}, CD8^{+} and CD56^{+} subsets indicate a coordinated checkpoint regulation within systemic immune compartment of IPF patients. This result mirrors checkpoint co-regulation observed in chronic viral infections and cancer, reinforcing the concept of "immune exhaustion" as a feature of IPF's immune landscape (108).

Interestingly, our PCA results revealed a clear segregation of IPF and HC samples, particularly under stimulated conditions, indicating disease-specific landscape. Our analysis highlights that IPF-derived CD8^{+} T cells maintain a stable inhibitory–activation signature mainly characterized by exhaustion and activation markers PD-1, TIGIT, CD25, and CD69 expression, when compared to drugs administration. This profile suggests that the exhausted phenotype of CD8^{+} T cells in IPF is not easily reversed by anti–PD-1, nintedanib, or their combination, consistent with evidence that PD-1/PD-L1 blockade in fibrotic lungs mainly affects fibroblast populations rather than reactivating T cells (99).

Persistent PD-1 expression despite treatment might also indicate the establishment of resistance mechanisms to checkpoint inhibition (109). Similarly, nintedanib, by targeting receptor tyrosine kinases for VEGF, FGF, and PDGF, may modulate cytokine production (IFN-γ, IL-2, IL-4, IL-10, IL-13) and reduce inflammatory signalling without directly enhancing T-cell activation (110).

Activation markers such as CD25 and CD69 exhibited altered trends in IPF patients compared with healthy controls, suggesting a dysregulated activation profile of $CD8^+$ T cells.

CD25 (IL-2Rα) a late activation marker regulated by IL-2 and PD-1 signalling, increased slightly after anti–PD-1 treatment but decreased with nintedanib and combination therapy, indicating a partial reactivation effect by PD-1 blockade counterbalanced by the anti-fibrotic drug's inhibitory actions on fibroblast-driven cytokine networks (111) (112). This data suggests that anti-PD-1 stimulation might transiently "reignite" partially exhausted $CD8^+$ T cells in IPF, reflected by a modest increase in CD25, whereas nintedanib (113) (26), could indirectly suppress T-cell activation. In HCs, by contrast, CD25 levels were higher at baseline and decreased after treatment, consistent with a well-regulated immune system where PD-1 blockade does not lead to pathological activation. . These results underlines how immune reactivation in IPF may differ from that in physiological conditions.

The other activation markers analysed, CD69, that consists in an early activation marker involved in lymphocyte retention T cells in tissues (114) , decreased after anti–PD-1 but increased after nintedanib and combination treatment, suggesting opposing modulation of immune activation and trafficking dynamics. These patterns mirror reports in non–small cell lung cancer linking CD69 expression with pre-exhausted $CD8^+$ T cells that retain partial effector functions but display dysfunction (115) (116) . Conversely, nintedanib and the combination treatment shows an increased trend in CD69 expression, implying an effect consistent with local retention or reactivation, likely linked to its modulation of fibrotic and cytokine signalling pathways (110) . The combination of anti-PD-1 and nintedanib induced an increase of CD69 expression on $CD8^+$ T cells, indicating a synergistic effect between the treatments. Such synergy is biologically plausible given the distinct but intersecting roles of these agents in immune checkpoint and fibrotic signalling pathways that influence T-cell activation.

This parallel supports the hypothesis that, in IPF, chronic inflammation and fibrosis drive an ineffective activation state, reflected in the aberrant regulation of both early (CD69) and late (CD25) activation markers.

Furthermore, the analysis of PD-1 and TIGIT expression reinforces the notion of complex inhibitory regulation in IPF. In HCs, as expected PD-1 expression decreased following anti-PD-1 treatment, while nintedanib increased PD-1 levels, and the combination further enhanced them. In contrast, IPF-derived $CD8^+$ T cells, anti-PD-1failed to reduce PD-1 expression, and in some cases further increased it. This paradox has been explained in literature, although without clear demonstration of this phenomenon (117) (109). Moreover, the inhibition of specific immune checkpoints with the use of checkpoint inhibitors can lead to the compensatory activation of alternative immune checkpoints, thereby contributing to resistance (117). According to this study, we noted elevated TIGIT expression regardless of treatment, suggesting a cooperative inhibitory effect between TIGIT and PD-1. Furthermore, studies in NSCLC showed that TIGIT is induced earlier than PD-1 during $CD8^+$ T-cell activation and marks a pre-exhausted state enriched for $PD\text{-}1^+$ cells, displaying compromised effector function (105). In line with this study, our results suggest that TIGIT may act as an early inhibitory "brake" during $CD8^+$ T-cell activation and exhaustion, predisposing cells to subsequent PD-1–mediated suppression. The dysregulation of CD25 and CD69, in parallel with persistent PD-1 and TIGIT expression, supports a model comprises $CD8^+$ T cells dysfunctional activation state, unable to mount effective responses due to redundant inhibitory signalling and chronic activation.

Regarding the cytotoxic markers, controversial results were reported in literature. Our data showed a reduction of Granzyme B in IPF patient. Nintedanib treatment significantly increased its expression, while anti–PD-1 and combination therapy further reduced it. This suggests that PD-1 blockade alone fails to restore effective cytotoxicity in IPF. Prior studies showing reduced Granzyme B release in IPF $CD8^+$ T cells upon strong stimuli such as CMV infection (118). These data are in line with our previous described observations of dysregulated activation markers (CD25, CD69) and persistent expression of exhaustion markers (PD-1, TIGIT). Taken together our results suggesting that IPF $CD8^+$ T cells are functionally impaired and unable to regain full effector function despite exogenous stimulation. Reduced Granzyme B has also been associated with poor outcomes in cancer (119) .By contrast, in HCs, Granzyme B levels decreased under treatment, consistent with a controlled immune responses: T-cell activation and

cytotoxicity are tightly regulated and checkpoint modulation does not lead to sustained activation.

As previously demonstrated, Granzyme B and Perforin expression are not strictly coupled (120) .Our data also reflect this independence: Perforin expression remained low across all treatments in both IPF and HCs (121) Furthermore, in oncological contexts insufficient Perforin levels have been correlated with disease progression and impaired immune surveillance (122) . This emphasize that reduced cytolytic capacity may be a shared feature of dysfunctional T-cell states in both cancer and fibrosis.

The degranulation markerLAMP-1 (CD107a) showed high in IPF samples, indicating ongoing degranulation or senescence (123) consistent with a chronic stimulatory environment that maintains partial activation without effective cytotoxicity. The persistence of LAMP-1 expression despite different treatments further suggests that neither anti–PD-1 nor nintedanib effectively reverse T-cell senescence, in agreement with our findings of sustained TIGIT expression and blunted activation responses. This pattern reflects a population of non-functional, chronically stimulated $CD8^+$ T cells. Conversely, in HCs, LAMP-1 expression decreased under all treatments compared with unstimulated cells indicating a preserved T-cell regulation of activation and subsequent return to quiescence, which is typically impaired in IPF.

Finally, ICAM-1 (CD54) expression showed a general decreasing trend under treatment in both IPF and control samples. This observation aligns with previous studies reporting elevated ICAM-1 in lung tissues and serum from IPF samples (124) . This result suggests that nintedanib and anti–PD-1 treatments may partially normalize T-cell adhesion and trafficking signals, potentially contributing to reduced inflammatory recruitment.

Functional assays confirmed reduced killing activity after treatment, particularly with anti–PD-1, whereas nintedanib and the combination of this drug with nintedanib produced modest recovery, consistent with incomplete functional restoration. Interestingly, proliferation assays showed that both anti–PD-1 and nintedanib increased $CD8^+$ T-cell proliferation, but the combination abolished this effect, suggesting interference between immune system and antifibrotic pathways. Samples from HCs showed an opposite trend, with decreased proliferation and cytotoxicity when treated, confirming that these effects are disease specific. In line with previous studies, nintedanib has been reported to

promote lymphocyte proliferation and metabolic activity without necessarily expanding total cell numbers, possibly by acting on fibroblast-derived cytokine networks or growth factor–related pathways that indirectly influence immune cell activation (110). Collectively, these results demonstrate a decoupling between proliferation and cytotoxicity in IPF $CD8^+$ T cells. These cells in fact proliferate and in the meanwhile fail to recover effector capacity—reflecting a hallmark of chronic immune dysfunction.

The absence of additive and/ or restorative effects from the combined anti–PD-1 and nintedanib treatment likely reflects multiple, non-exclusive mechanisms. First, PD-1 blockade and nintedanib act on distinct biological targets—immune checkpoint signalling versus fibroblast-driven tyrosine kinase pathways (FGFR, VEGFR, PDGFR)—that do not directly synergize and may yield antagonistic downstream effects depending on timing and cellular context (125). Second, persistent upregulation of alternative inhibitory receptors, notably TIGIT, may counterbalance PD-1 blockade and maintain functional exhaustion (117).

Moreover, chronic antigenic stimulation in IPF may induce senescent or terminally exhausted states in $CD8^+$ T cells that are not reversible through single checkpoint inhibition. . Furthermore, fibroblast-derived mediators such as TGF-β and IL-10, as well as metabolic constraints within the fibrotic microenvironment, can suppress T-cell function irrespective of PD-1 signalling. Finally, divergent results in the literature—including reports that pembrolizumab reduces PD-1/PD-L1 interaction primarily in $CD4^+$ T cells, while nivolumab can exacerbate fibrosis—underscore that immune checkpoint modulation in IPF is complex and context dependent (89) (126) . Overall, these observations suggest that the inhibition of a single checkpoint axis or isolated antifibrotic pathways is insufficient to restore immune competence in IPF, highlighting the need for multi-targeted and context-specific therapeutic strategies.

This study has some limitations. First, the sample size was relatively small, which may restrict the statistical power to detect subtle differences across treatment conditions and immune subsets. Second, the in vitro treatment model, while informative for mechanistic insights, may not fully reproduce the complex pharmacokinetic and cellular crosstalk occurring in vivo. Additionally, although we assessed a broad panel of activation, exhaustion, and cytotoxicity markers, the functional readouts were limited to short-term

stimulation and did not capture long-term differentiation, metabolic remodelling or cytokine secretion profiles. Finally, the study focused on the PD-1/TIGIT inhibitory axes and did not evaluate other potentially relevant checkpoints or immunomodulatory pathways—such as LAG-3, TIM-3, or metabolic regulators—which may contribute to resistance to immune reactivation.

6.1 Conclusion

Our findings provide new insights into the immune landscape of IPF. We demonstrate that systemic lymphocytes from IPF patients exhibit a state of chronic activation coupled with functional exhaustion, reflected in persistent PD-1 and TIGIT expression, dysregulated activation markers, and reduced cytotoxic potential. The lack of functional recovery following anti–PD-1, nintedanib, or combination treatment suggests that the exhausted phenotype in IPF is deeply imprinted and resistant to reversal through single or dual pathway modulation. Mechanistically, this may reflect the convergence of redundant inhibitory signalling, irreversible senescence, and suppressive cues from the fibrotic microenvironment.

6.2 Future Directions

Building on these findings, future research should explore the involvement of immune system during IPF progression. A possible use of combinatorial therapeutic strategies that simultaneously target multiple inhibitory checkpoints or integrate immune-modulating and antifibrotic mechanisms could be investigated. Dual blockade of PD-1 and TIGIT, or the inclusion of agents targeting metabolic and cytokine pathways such as TGF-β or IL-10, may offer the most effective treatment. Moreover, in vivo studies should delineate the cellular interactions underpinning immune exhaustion and fibrosis, guiding the development of personalized immunotherapeutic interventions tailored to the immunological phenotype of each patient.

Bibliography

1. Travis WD, Costabel U, Hansell DM, King TE, Lynch DA, Nicholson AG, et al. An Official American Thoracic Society/European Respiratory Society Statement: Update of the International Multidisciplinary Classification of the Idiopathic Interstitial Pneumonias. Am J Respir Crit Care Med. 2013 Sep 15;188(6):733–48.

2. Ryerson CJ, Adegunsoye A, Piciucchi S, Hariri LP, Khor YH, Wijsenbeek MS, et al. Update of the International Multidisciplinary Classification of the Interstitial Pneumonias: An ERS/ATS Statement. European Respiratory Journal [Internet]. 2025 Aug 28 [cited 2025 Oct 22]; Available from: https://publications.ersnet.org/content/erj/early/2025/08/21/13993003.00158-2025

3. Dsouza K, de Andrade JA. The Diagnostic Approach to Interstitial Lung Disease. Curr Pulmonol Rep. 2018 Dec 1;7(4):149–59.

4. Plantier L, Cazes A, Dinh-Xuan AT, Bancal C, Marchand-Adam S, Crestani B. Physiology of the lung in idiopathic pulmonary fibrosis. Eur Respir Rev. 2018 Mar 31;27(147):170062.

5. Goldin J, Cascella M. Diffusing Capacity of the Lungs for Carbon Monoxide. In: StatPearls [Internet]. Treasure Island (FL): StatPearls Publishing; 2025 [cited 2025 Oct 22]. Available from: http://www.ncbi.nlm.nih.gov/books/NBK556149/

6. Raghu G, Remy-Jardin M, Richeldi L, Thomson CC, Inoue Y, Johkoh T, et al. Idiopathic Pulmonary Fibrosis (an Update) and Progressive Pulmonary Fibrosis in Adults: An Official ATS/ERS/JRS/ALAT Clinical Practice Guideline. Am J Respir Crit Care Med. 2022 May 1;205(9):e18–47.

7. Koudstaal T, Wijsenbeek MS. Idiopathic pulmonary fibrosis. La Presse Médicale. 2023 Sep 1;52(3):104166.

8. León-Román F, Valenzuela C, Molina-Molina M. Idiopathic pulmonary fibrosis. Medicina Clínica (English Edition). 2022 Aug 26;159(4):189–94.

9. Liu RM, Liu G. Cell senescence and fibrotic lung diseases. Exp Gerontol. 2020 Apr;132:110836.

10. Gribbin J, Hubbard RB, Le Jeune I, Smith CJP, West J, Tata LJ. Incidence and mortality of idiopathic pulmonary fibrosis and sarcoidosis in the UK. Thorax. 2006 Nov;61(11):980–5.

11. Phan THG, Paliogiannis P, Nasrallah GK, Giordo R, Eid AH, Fois AG, et al. Emerging cellular and molecular determinants of idiopathic pulmonary fibrosis. Cell Mol Life Sci. 2021 Mar 1;78(5):2031–57.

12. Rivera-Ortega P, Molina-Molina M. Interstitial Lung Diseases in Developing Countries. Annals of Global Health [Internet]. 2019 Jan 22 [cited 2025 Oct 22];85(1). Available from: https://annalsofglobalhealth.org/articles/10.5334/aogh.2414

13. Seibold MA, Wise AL, Speer MC, Steele MP, Brown KK, Loyd JE, et al. A Common MUC5B Promoter Polymorphism and Pulmonary Fibrosis. New England Journal of Medicine. 2011 Apr 21;364(16):1503–12.

14. Noth I, Zhang Y, Ma SF, Flores C, Barber M, Huang Y, et al. Genetic variants associated with idiopathic pulmonary fibrosis susceptibility and mortality: a genome-wide association study. Lancet Respir Med. 2013 Jun;1(4):309–17.

15. Lawson WE, Grant SW, Ambrosini V, Womble KE, Dawson EP, Lane KB, et al. Genetic mutations in surfactant protein C are a rare cause of sporadic cases of IPF. Thorax. 2004 Nov;59(11):977–80.

16. Wang Y, Kuan PJ, Xing C, Cronkhite JT, Torres F, Rosenblatt RL, et al. Genetic defects in surfactant protein A2 are associated with pulmonary fibrosis and lung cancer. Am J Hum Genet. 2009 Jan;84(1):52–9.

17. Allen RJ, Porte J, Braybrooke R, Flores C, Fingerlin TE, Oldham JM, et al. Genetic variants associated with susceptibility to idiopathic pulmonary fibrosis in people of European ancestry: a genome-wide association study. The Lancet Respiratory Medicine. 2017 Nov 1;5(11):869–80.

18. Stuart BD, Choi J, Zaidi S, Xing C, Holohan B, Chen R, et al. Exome sequencing links mutations in PARN and RTEL1 with familial pulmonary fibrosis and telomere shortening. Nat Genet. 2015 May;47(5):512–7.

19. Raghu G, Collard HR, Egan JJ, Martinez FJ, Behr J, Brown KK, et al. An Official ATS/ERS/JRS/ALAT Statement: Idiopathic Pulmonary Fibrosis: Evidence-based Guidelines for Diagnosis and Management. Am J Respir Crit Care Med. 2011 Mar 15;183(6):788–824.

20. Raghu G, Remy-Jardin M, Myers JL, Richeldi L, Ryerson CJ, Lederer DJ, et al. Diagnosis of Idiopathic Pulmonary Fibrosis. An Official ATS/ERS/JRS/ALAT Clinical Practice Guideline. Am J Respir Crit Care Med. 2018 Sep 1;198(5):e44–68.

21. Podolanczuk AJ, Thomson CC, Remy-Jardin M, Richeldi L, Martinez FJ, Kolb M, et al. Idiopathic pulmonary fibrosis: state of the art for 2023. European Respiratory Journal [Internet]. 2023 Apr 20 [cited 2025 Oct 22];61(4). Available from: https://publications.ersnet.org/content/erj/61/4/2200957

22. Azuma A, Nukiwa T, Tsuboi E, Suga M, Abe S, Nakata K, et al. Double-blind, Placebo-controlled Trial of Pirfenidone in Patients with Idiopathic Pulmonary Fibrosis. Am J Respir Crit Care Med. 2005 May;171(9):1040–7.

23. Myllärniemi M, Kaarteenaho R. Pharmacological treatment of idiopathic pulmonary fibrosis – preclinical and clinical studies of pirfenidone, nintedanib, and N-acetylcysteine. European Clinical Respiratory Journal. 2015 Jan 1;2(1):26385.

24. McCormack PL. Nintedanib: first global approval. Drugs. 2015 Jan;75(1):129–39.

25. Hilberg F, Roth GJ, Krssak M, Kautschitsch S, Sommergruber W, Tontsch-Grunt U, et al. BIBF 1120: triple angiokinase inhibitor with sustained receptor blockade and good antitumor efficacy. Cancer Res. 2008 Jun 15;68(12):4774–82.

26. Wollin L, Wex E, Pautsch A, Schnapp G, Hostettler KE, Stowasser S, et al. Mode of action of nintedanib in the treatment of idiopathic pulmonary fibrosis. European Respiratory Journal. 2015 Apr 30;45(5):1434–45.

27. Richeldi L, du Bois RM, Raghu G, Azuma A, Brown KK, Costabel U, et al. Efficacy and safety of nintedanib in idiopathic pulmonary fibrosis. N Engl J Med. 2014 May 29;370(22):2071–82.

28. Roth GJ, Binder R, Colbatzky F, Dallinger C, Schlenker-Herceg R, Hilberg F, et al. Nintedanib: from discovery to the clinic. J Med Chem. 2015 Feb 12;58(3):1053–63.

29. Wollin L, Maillet I, Quesniaux V, Holweg A, Ryffel B. Antifibrotic and anti-inflammatory activity of the tyrosine kinase inhibitor nintedanib in experimental models of lung fibrosis. J Pharmacol Exp Ther. 2014 May;349(2):209–20.

30. Crestani B, Huggins JT, Kaye M, Costabel U, Glaspole I, Ogura T, et al. Long-term safety and tolerability of nintedanib in patients with idiopathic pulmonary fibrosis: results from the open-label extension study, INPULSIS-ON. The Lancet Respiratory Medicine. 2019 Jan 1;7(1):60–8.

31. Flaherty KR, Wells AU, Cottin V, Devaraj A, Walsh SLF, Inoue Y, et al. Nintedanib in Progressive Fibrosing Interstitial Lung Diseases. New England Journal of Medicine. 2019 Oct 31;381(18):1718–27.

32. Bonella F, Spagnolo P, Ryerson C. Current and Future Treatment Landscape for Idiopathic Pulmonary Fibrosis. Drugs. 2023 Nov;83(17):1581–93.

33. Spagnolo P, Maher TM. The future of clinical trials in idiopathic pulmonary fibrosis. Curr Opin Pulm Med. 2024 Sep 1;30(5):494–9.

34. Libra A, Sciacca E, Muscato G, Sambataro G, Spicuzza L, Vancheri C. Highlights on Future Treatments of IPF: Clues and Pitfalls. International Journal of Molecular Sciences. 2024 Jan;25(15):8392.

35. U.S. Food and Drug Administration [Internet]. [cited 2025 Oct 22]. FDA Approves Drug to Treat Idiopathic Pulmonary Fibrosis. Available from: https://content.govdelivery.com/accounts/USFDA/bulletins/3f61959

36. Nerandomilast in Patients with Idiopathic Pulmonary Fibrosis | New England Journal of Medicine [Internet]. [cited 2025 Oct 22]. Available from: https://www.nejm.org/doi/full/10.1056/NEJMoa2414108

37. Bringardner BD, Baran CP, Eubank TD, Marsh CB. The role of inflammation in the pathogenesis of idiopathic pulmonary fibrosis. Antioxid Redox Signal. 2008 Feb;10(2):287–301.

38. Chambers RC, Mercer PF. Mechanisms of alveolar epithelial injury, repair, and fibrosis. Ann Am Thorac Soc. 2015 Mar;12 Suppl 1(Suppl 1):S16-20.

39. Salton F, Volpe MC, Confalonieri M. Epithelial–Mesenchymal Transition in the Pathogenesis of Idiopathic Pulmonary Fibrosis. Medicina (Kaunas). 2019 Mar 28;55(4):83.

40. du Bois RM. Fibroblastic Foci: Time To Be Counted? Chest. 2006 Jul 1;130(1):3–5.

41. Cool CD, Groshong SD, Rai PR, Henson PM, Stewart JS, Brown KK. Fibroblast foci are not discrete sites of lung injury or repair: the fibroblast reticulum. Am J Respir Crit Care Med. 2006 Sep 15;174(6):654–8.

42. Selman M, King TE, Pardo A, American Thoracic Society, European Respiratory Society, American College of Chest Physicians. Idiopathic pulmonary fibrosis: prevailing and evolving hypotheses about its pathogenesis and implications for therapy. Ann Intern Med. 2001 Jan 16;134(2):136–51.

43. Liu GY, Budinger GRS, Dematte JE. Advances in the management of idiopathic pulmonary fibrosis and progressive pulmonary fibrosis. 2022 Jun 29 [cited 2025 Oct 22]; Available from: https://www.bmj.com/content/377/bmj-2021-066354

44. Wolters PJ, Collard HR, Jones KD. Pathogenesis of Idiopathic Pulmonary Fibrosis. Annu Rev Pathol. 2014;9:157–79.

45. Pokhreal D, Crestani B, Helou DG. Macrophage Implication in IPF: Updates on Immune, Epigenetic, and Metabolic Pathways. Cells. 2023 Sep 1;12(17):2193.

46. Martinez FJ, Chisholm A, Collard HR, Flaherty KR, Myers J, Raghu G, et al. The diagnosis of idiopathic pulmonary fibrosis: current and future approaches. Lancet Respir Med. 2017 Jan;5(1):61–71.

47. Zhang J, Xu X, Liang Y, Wu X, Qian Z, Zhang L, et al. Particulate matter promotes the epithelial to mesenchymal transition in human lung epithelial cells via the ROS pathway. Am J Transl Res. 2023;15(8):5159–67.

48. Ju X, Wang K, Wang C, Zeng C, Wang Y, Yu J. Regulation of myofibroblast dedifferentiation in pulmonary fibrosis. Respiratory Research. 2024 Jul 18;25(1):284.

49. Shenderov K, Collins SL, Powell JD, Horton MR. Immune dysregulation as a driver of idiopathic pulmonary fibrosis. J Clin Invest [Internet]. 2021 Jan 19 [cited 2025 Oct 22];131(2). Available from: https://www.jci.org/articles/view/143226

50. Kageyama T, Ito T, Tanaka S, Nakajima H. Physiological and immunological barriers in the lung. Semin Immunopathol. 2024 Jan;45(4–6):533–47.

51. Georas SN, Upham J. Environmental exposures and innate immunity in the lung. J Environ Immunol Toxicol. 2014;2(1):1–3.

52. Gopallawa I, Dehinwal R, Bhatia V, Gujar V, Chirmule N. A four-part guide to lung immunology: Invasion, inflammation, immunity, and intervention. Front Immunol [Internet]. 2023 Mar 31 [cited 2025 Oct 22];14. Available from: https://www.frontiersin.org/journals/immunology/articles/10.3389/fimmu.2023.1119564/full

53. Chrysanthopoulou A, Mitroulis I, Apostolidou E, Arelaki S, Mikroulis D, Konstantinidis T, et al. Neutrophil extracellular traps promote differentiation and function of fibroblasts. J Pathol. 2014 Jul;233(3):294–307.

54. Gregory AD, Kliment CR, Metz HE, Kim KH, Kargl J, Agostini BA, et al. Neutrophil elastase promotes myofibroblast differentiation in lung fibrosis. J Leukoc Biol. 2015 Aug;98(2):143–52.

55. Kinder BW, Brown KK, Schwarz MI, Ix JH, Kervitsky A, King TE. Baseline BAL neutrophilia predicts early mortality in idiopathic pulmonary fibrosis. Chest. 2008 Jan;133(1):226–32.

56. Zhang L, Wang Y, Wu G, Xiong W, Gu W, Wang CY. Macrophages: friend or foe in idiopathic pulmonary fibrosis? Respir Res. 2018 Sep 6;19(1):170.

57. Mitsi E, Kamng'ona R, Rylance J, Solórzano C, Jesus Reiné J, Mwandumba HC, et al. Human alveolar macrophages predominately express combined classical M1 and M2 surface markers in steady state. Respir Res. 2018 Apr 18;19(1):66.

58. Choi SM, Mo Y, Bang JY, Ko YG, Ahn YH, Kim HY, et al. Classical monocyte-derived macrophages as therapeutic targets of umbilical cord mesenchymal stem cells: comparison of intratracheal and intravenous administration in a mouse model of pulmonary fibrosis. Respir Res. 2023 Mar 5;24(1):68.

59. Desai O, Winkler J, Minasyan M, Herzog EL. The Role of Immune and Inflammatory Cells in Idiopathic Pulmonary Fibrosis. Front Med (Lausanne). 2018;5:43.

60. Reinhardt JW, Breuer CK. Fibrocytes: A Critical Review and Practical Guide. Front Immunol. 2021;12:784401.

61. Zoso A, Mazza EMC, Bicciato S, Mandruzzato S, Bronte V, Serafini P, et al. Human fibrocytic myeloid-derived suppressor cells express IDO and promote tolerance via Treg-cell expansion. Eur J Immunol. 2014 Nov;44(11):3307–19.

62. Horsburgh S, Todryk S, Ramming A, Distler JHW, O'Reilly S. Innate lymphoid cells and fibrotic regulation. Immunol Lett. 2018 Mar;195:38–44.

63. Jacquelot N, Seillet C, Vivier E, Belz GT. Innate lymphoid cells and cancer. Nat Immunol. 2022 Mar;23(3):371–9.

64. Heukels P, Moor CC, von der Thüsen JH, Wijsenbeek MS, Kool M. Inflammation and immunity in IPF pathogenesis and treatment. Respir Med. 2019 Feb;147:79–91.

65. Liu H, Jakubzick C, Osterburg AR, Nelson RL, Gupta N, McCormack FX, et al. Dendritic Cell Trafficking and Function in Rare Lung Diseases. Am J Respir Cell Mol Biol. 2017 Oct;57(4):393–402.

66. Gong P, Lu Y, Chai X, Li X. Exploring the Causal Relationship Between Immune Cells and Idiopathic Pulmonary Fibrosis: A Mendelian Randomization Analysis. Journal of Clinical Laboratory Analysis. 2025;39(8):e70026.

67. Cruz T, Jia M, Sembrat J, Tabib T, Agostino N, Bruno TC, et al. Reduced Proportion and Activity of Natural Killer Cells in the Lung of Patients with Idiopathic Pulmonary Fibrosis. Am J Respir Crit Care Med. 2021 Sep;204(5):608–10.

68. Esposito I, Perna F, Ponticiello A, Perrella M, Gilli M, Sanduzzi A. Natural killer cells in Bal and peripheral blood of patients with idiopathic pulmonary fibrosis (IPF). Int J Immunopathol Pharmacol. 2005;18(3):541–5.

69. Kumar V, Hertz M, Agro A, Byrne AJ. Type 1 invariant natural killer T cells in chronic inflammation and tissue fibrosis. Front Immunol [Internet]. 2023 Sep 25 [cited 2025 Oct 22];14. Available from: https://www.frontiersin.org/journals/immunology/articles/10.3389/fimmu.2023.1260503/full

70. Cruz T, Agudelo Garcia PA, Chamucero-Millares JA, Bondonese A, Mitash N, Sembrat J, et al. End-Stage Idiopathic Pulmonary Fibrosis Lung Microenvironment Promotes Impaired NK Activity. J Immunol. 2023 Oct 1;211(7):1073–81.

71. Bergantini L, d'Alessandro M, Cameli P, Otranto A, Finco T, Curatola G, et al. Prognostic role of NK cell percentages in bronchoalveolar lavage from patients with different fibrotic interstitial lung diseases. Clin Immunol. 2021 Sep;230:108827.

72. Luzina IG, Todd NW, Iacono AT, Atamas SP. Roles of T lymphocytes in pulmonary fibrosis. J Leukoc Biol. 2008 Feb;83(2):237–44.

73. Deng L, Huang T, Zhang L. T cells in idiopathic pulmonary fibrosis: crucial but controversial. Cell Death Discov. 2023 Feb 14;9(1):62.

74. Deng L, Huang T, Zhang L. Correction to: T cells in idiopathic pulmonary fibrosis: crucial but controversial. Cell Death Discov. 2023 Feb 23;9(1):74.

75. Quezada SA, Jarvinen LZ, Lind EF, Noelle RJ. CD40/CD154 interactions at the interface of tolerance and immunity. Annu Rev Immunol. 2004;22:307–28.

76. Feghali-Bostwick CA, Tsai CG, Valentine VG, Kantrow S, Stoner MW, Pilewski JM, et al. Cellular and humoral autoreactivity in idiopathic pulmonary fibrosis. J Immunol. 2007 Aug 15;179(4):2592–9.

77. Majchrzak K, Nelson MH, Bailey SR, Bowers JS, Yu XZ, Rubinstein MP, et al. Exploiting IL-17-producing CD4+ and CD8+ T cells to improve cancer immunotherapy in the clinic. Cancer Immunol Immunother. 2016 Mar;65(3):247–59.

78. Wynn TA. Fibrotic disease and the T(H)1/T(H)2 paradigm. Nat Rev Immunol. 2004 Aug;4(8):583–94.

79. Liu H, Cui H, Liu G. The Intersection between Immune System and Idiopathic Pulmonary Fibrosis-A Concise Review. Fibrosis (Hong Kong). 2025;3(1):10004.

80. Xu Y, Lan P, Wang T. The Role of Immune Cells in the Pathogenesis of Idiopathic Pulmonary Fibrosis. Medicina. 2023 Nov;59(11):1984.

81. Wilson MS, Madala SK, Ramalingam TR, Gochuico BR, Rosas IO, Cheever AW, et al. Bleomycin and IL-1β–mediated pulmonary fibrosis is IL-17A dependent. J Exp Med. 2010 Feb 22;207(3):535–52.

82. Zhang J, Wang D, Wang L, Wang S, Roden AC, Zhao H, et al. Profibrotic effect of IL-17A and elevated IL-17RA in idiopathic pulmonary fibrosis and rheumatoid arthritis-associated lung disease support a direct role for IL-17A/IL-17RA in human fibrotic interstitial lung disease. American Journal of Physiology-Lung Cellular and Molecular Physiology. 2019 Mar;316(3):L487–97.

83. Lo Re S, Lecocq M, Uwambayinema F, Yakoub Y, Delos M, Demoulin JB, et al. Platelet-derived growth factor-producing CD4+ Foxp3+ regulatory T lymphocytes promote lung fibrosis. Am J Respir Crit Care Med. 2011 Dec 1;184(11):1270–81.

84. Reilkoff RA, Peng H, Murray LA, Peng X, Russell T, Montgomery R, et al. Semaphorin 7a+ regulatory T cells are associated with progressive idiopathic pulmonary fibrosis and are implicated in transforming growth factor-β1-induced pulmonary fibrosis. Am J Respir Crit Care Med. 2013 Jan 15;187(2):180–8.

85. Daniil Z, Kitsanta P, Kapotsis G, Mathioudaki M, Kollintza A, Karatza M, et al. CD8+ T lymphocytes in lung tissue from patients with idiopathic pulmonary fibrosis. Respir Res. 2005 Jul 24;6(1):81.

86. Feng X, Yu F, He XL, Cheng PP, Niu Q, Zhao LQ, et al. CD8+ tissue-resident memory T cells are essential in bleomycin-induced pulmonary fibrosis. Am J Physiol Cell Physiol. 2024 Nov 1;327(5):C1178–91.

87. Alexandrova Y, Yero A, Olivenstein R, Orlova M, Schurr E, Estaquier J, et al. Dynamics of pulmonary mucosal cytotoxic CD8 T-cells in people living with HIV under suppressive antiretroviral therapy. Respir Res. 2024 Jun 12;25(1):240.

88. Mutlu S, Fytianos K, Ferrié C, Scalise M, Mykoniati S, Gazdhar A, et al. Adoptive Transfer of T Cells as a Potential Therapeutic Approach in the Bleomycin-Injured Mouse Lung. J Gene Med. 2025 Apr;27(4):e70018.

89. Karampitsakos T, Galaris A, Chrysikos S, Papaioannou O, Vamvakaris I, Barbayianni I, et al. Expression of PD-1/PD-L1 axis in mediastinal lymph nodes and lung tissue of human and experimental lung fibrosis indicates a potential therapeutic target for idiopathic pulmonary fibrosis. Respir Res. 2023 Nov 14;24(1):279.

90. Orabona C, Mondanelli G, Puccetti P, Grohmann U. Immune Checkpoint

Molecules, Personalized Immunotherapy, and Autoimmune Diabetes. Trends Mol Med. 2018 Nov;24(11):931–41.

91. Palafox-Sánchez CA, Chávez-Mireles R, Salazar-Camarena DC, Palafox-Sánchez CA. Exploring the Role of PD-1 in the Autoimmune Response: Insights into Its Implication in Systemic Lupus Erythematosus [Internet]. Preprints; 2024 [cited 2025 Oct 23]. Available from: https://www.preprints.org/manuscript/202406.1533

92. Keir ME, Butte MJ, Freeman GJ, Sharpe AH. PD-1 and its ligands in tolerance and immunity. Annu Rev Immunol. 2008;26:677–704.

93. Kim MJ, Ha SJ. Differential Role of PD-1 Expressed by Various Immune and Tumor Cells in the Tumor Immune Microenvironment: Expression, Function, Therapeutic Efficacy, and Resistance to Cancer Immunotherapy. Front Cell Dev Biol [Internet]. 2021 Nov 22 [cited 2025 Oct 23];9. Available from: https://www.frontiersin.org/journals/cell-and-developmental-biology/articles/10.3389/fcell.2021.767466/full

94. Zhao Y, Qu Y, Hao C, Yao W. PD-1/PD-L1 axis in organ fibrosis. Front Immunol. 2023;14:1145682.

95. Zhou S, Zhu J, Xu J, Gu B, Zhao Q, Luo C, et al. Anti-tumour potential of PD-L1/PD-1 post-translational modifications. Immunology. 2022;167(4):471–81.

96. Jiang A, Liu N, Wang J, Zheng X, Ren M, Zhang W, et al. The role of PD-1/PD-L1 axis in idiopathic pulmonary fibrosis: Friend or foe? Front Immunol. 2022;13:1022228.

97. Cui L, Chen SY, Lerbs T, Lee JW, Domizi P, Gordon S, et al. Activation of JUN in fibroblasts promotes pro-fibrotic programme and modulates protective immunity. Nat Commun. 2020 Jun 3;11(1):2795.

98. Duitman J, van den Ende T, Spek CA. Immune Checkpoints as Promising Targets for the Treatment of Idiopathic Pulmonary Fibrosis? Journal of Clinical Medicine. 2019 Oct;8(10):1547.

99. Tan J, Xue Q, Hu X, Yang J. Inhibitor of PD-1/PD-L1: a new approach may be beneficial for the treatment of idiopathic pulmonary fibrosis. Journal of Translational Medicine. 2024 Jan 23;22(1):95.

100. Lederer DJ, Martinez FJ. Idiopathic Pulmonary Fibrosis. N Engl J Med. 2018 May 10;378(19):1811–23.

101. Hewitt RJ, Maher TM. Idiopathic Pulmonary Fibrosis: New and Emerging Treatment Options. Drugs Aging. 2019 Jun;36(6):485–92.

102. Todd NW, Scheraga RG, Galvin JR, Iacono AT, Britt EJ, Luzina IG, et al. Lymphocyte aggregates persist and accumulate in the lungs of patients with idiopathic pulmonary fibrosis. J Inflamm Res. 2013;6:63–70.

103. Celada LJ, Kropski JA, Herazo-Maya JD, Luo W, Creecy A, Abad AT, et al. PD-1 up-regulation on CD4+ T cells promotes pulmonary fibrosis through STAT3-mediated IL-17A and TGF-β1 production. Sci Transl Med. 2018 Sep 26;10(460):eaar8356.

104. Ni K, Liu M, Zheng J, Wen L, Chen Q, Xiang Z, et al. PD-1/PD-L1 Pathway Mediates the Alleviation of Pulmonary Fibrosis by Human Mesenchymal Stem Cells in Humanized Mice. Am J Respir Cell Mol Biol. 2018 Jun;58(6):684–95.

105. Hu F, Wang W, Fang C, Bai C. TIGIT presents earlier expression dynamic than PD-1 in activated CD8+ T cells and is upregulated in non-small cell lung cancer patients. Exp Cell Res. 2020 Nov 1;396(1):112260.

106. Yang L, Zhang Y, Yang L. Adenosine signaling in tumor-associated macrophages and targeting adenosine signaling for cancer therapy. Cancer Biol Med. 2024 Nov 15;21(11):995–1011.

107. Pauken KE, Wherry EJ. Overcoming T cell exhaustion in infection and cancer. Trends Immunol. 2015 Apr;36(4):265–76.

108. Wherry EJ, Kurachi M. Molecular and cellular insights into T cell exhaustion. Nat Rev Immunol. 2015 Aug;15(8):486–99.

109. Vesely MD, Zhang T, Chen L. Resistance Mechanisms to Anti-PD Cancer Immunotherapy. Annu Rev Immunol. 2022 Apr 26;40:45–74.

110. Ubieta K, Thomas MJ, Wollin L. The Effect of Nintedanib on T-Cell Activation, Subsets and Functions. Drug Des Devel Ther. 2021;15:997–1011.

111. Beltra JC, Manne S, Abdel-Hakeem MS, Kurachi M, Giles JR, Chen Z, et al. Developmental Relationships of Four Exhausted CD8+ T Cell Subsets Reveals Underlying Transcriptional and Epigenetic Landscape Control Mechanisms. Immunity. 2020 May 19;52(5):825-841.e8.

112. Liu R, Li HF, Li S. PD-1-mediated inhibition of T cell activation: Mechanisms and strategies for cancer combination immunotherapy. Cell Insight. 2024 Apr 1;3(2):100146.

113. Hostettler KE, Zhong J, Papakonstantinou E, Karakiulakis G, Tamm M, Seidel P, et al. Anti-fibrotic effects of nintedanib in lung fibroblasts derived from patients with idiopathic pulmonary fibrosis. Respir Res. 2014 Dec 12;15(1):157.

114. Cibrián D, Sánchez-Madrid F. CD69: from activation marker to metabolic gatekeeper. Eur J Immunol. 2017 Jun;47(6):946–53.

115. Hu ZW, Sun W, Wen YH, Ma RQ, Chen L, Chen WQ, et al. CD69 and SBK1 as potential predictors of responses to PD-1/PD-L1 blockade cancer immunotherapy in lung cancer and melanoma. Front Immunol [Internet]. 2022 Aug 15 [cited 2025 Oct 23];13. Available from: https://www.frontiersin.org/journals/immunology/articles/10.3389/fimmu.2022.9520

59/full

116. Li Y, Gu Y, Yang P, Wang Y, Yu X, Li Y, et al. CD69 is a Promising Immunotherapy and Prognosis Prediction Target in Cancer. ITT. 2024 Jan 9;13:1–14.

117. Gao P, Li X, Duan Z, Wang Y, Li Y, Wang J, et al. Improvement of the Anticancer Efficacy of PD-1/PD-L1 Blockade: Advances in Molecular Mechanisms and Therapeutic Strategies. MedComm (2020). 2025 Aug;6(8):e70274.

118. Nowacki TM, Kuerten S, Zhang W, Shive CL, Kreher CR, Boehm BO, et al. Granzyme B production distinguishes recently activated CD8(+) memory cells from resting memory cells. Cell Immunol. 2007 May;247(1):36–48.

119. Hurkmans DP, Basak EA, Schepers N, Oomen-De Hoop E, Van der Leest CH, El Bouazzaoui S, et al. Granzyme B is correlated with clinical outcome after PD-1 blockade in patients with stage IV non-small-cell lung cancer. J Immunother Cancer. 2020 May;8(1):e000586.

120. Thompson R, Cao X. Reassessing granzyme B: unveiling perforin-independent versatility in immune responses and therapeutic potentials. Front Immunol. 2024;15:1392535.

121. Miyazaki H, Kuwano K, Yoshida K, Maeyama T, Yoshimi M, Fujita M, et al. The perforin mediated apoptotic pathway in lung injury and fibrosis. J Clin Pathol. 2004 Dec;57(12):1292–8.

122. Ota T, Fukui T, Nakahara Y, Takeda T, Uchino J, Mouri T, et al. Serum immune modulators during the first cycle of anti-PD-1 antibody therapy in non-small cell lung cancer: Perforin as a biomarker. Thorac Cancer. 2020 Nov;11(11):3223–33.

123. Meca-Laguna G, Qiu M, Hou Y, Barkovskaya A, Shankar A, Dixit B, et al. Cell-Surface LAMP1 is a Senescence Marker in Aging and Idiopathic Pulmonary Fibrosis. Aging Cell. 2025;24(9):e70141.

124. Okuda R, Matsushima H, Aoshiba K, Oba T, Kawabe R, Honda K, et al. Soluble intercellular adhesion molecule-1 for stable and acute phases of idiopathic pulmonary fibrosis. Springerplus. 2015;4:657.

125. Tu J, Xu H, Ma L, Li C, Qin W, Chen X, et al. Nintedanib enhances the efficacy of PD-L1 blockade by upregulating MHC-I and PD-L1 expression in tumor cells. Theranostics. 2022 Jan 1;12(2):747–66.

126. Duchemann B, Didier M, Pailler MC, Brillet PY, Kambouchner M, Uzunhan Y, et al. [Can nivolumab be used safely in idiopathic pulmonary fibrosis?]. Rev Mal Respir. 2019 Feb;36(2):209–13.